We are IntechOpen,
the world's leading publisher of
Open Access books
Built by scientists, for scientists

4,900
Open access books available

124,000
International authors and editors

140M
Downloads

154
Countries delivered to

Our authors are among the

TOP 1%
most cited scientists

12.2%
Contributors from top 500 universities

BOOK CITATION INDEX
CLARIVATE ANALYTICS
INDEXED

WEB OF SCIENCE™

Selection of our books indexed in the Book Citation Index
in Web of Science™ Core Collection (BKCI)

Interested in publishing with us?
Contact book.department@intechopen.com

Numbers displayed above are based on latest data collected.
For more information visit www.intechopen.com

Multiple Access Network Optimization Aspects via Swarm Search Algorithms

Taufik Abrão[1], Lucas Hiera Dias Sampaio[2], Mario Lemes Proença Jr.[3], Bruno Augusto Angélico[4] and Paul Jean E. Jeszensky[5]

[1,2,3]*State University of Londrina (UEL), Londrina, PR*
[4]*Federal University of Technology (UTFPR), Cornélio Procópio, PR*
[5]*Polytechnic School of University of Sao Paulo (EPUSP), São Paulo, SP*
Brazil

1. Introduction

In the current telecommunication scenario, companies must deal with spectrum scarcity, power consumption issues, increasing throughput demand, and quality of service (QoS) requirements, including high performance (in terms of bit error rate (BER)) with guarantees of delivering the target information rate per user-class, maximum allowed delay, and so on. In these situations, many optimization problems arise, such as multiuser detection and resource allocation.

A lot of innovative algorithms conception and research efforts have been spent in order to satisfy the new services requirements, such as growing capacity, availability, mobility, and multiclass services (i.e., multirate users) with different quality of service (QoS). Hence, inspired by this scenario, a different optimization approach based on heuristic procedures has been investigated.

Particle swarm optimization (PSO) was developed after some researchers have analyzed the birds behavior and discerning that the advantage obtained through their group life could be explored as a tool for a heuristic search. Considering this new concept of interaction among individuals, J. Kennedy and R. Eberhart developed a new heuristic search based on a particle swarm Kennedy & Eberhart (1995). The PSO principle is the movement of a group of particles, randomly distributed in the search space, each one with its own position and velocity. The position of each particle is modified by the application of velocity in order to reach a better performance. The interaction among particles is inserted in the calculation of particle velocity. In a multiple access DS/CDMA system, a conventional detector by itself may not provide a desirable performance and quality of service, once the system capacity is strongly affected by multiple access interference (MAI). The capacity of a DS/CDMA system in multipath channels is limited mainly by the MAI, self-interference (SI), near-far effect (NFR) and fading. The conventional receiver for multipath channels (Rake receiver) explores the path diversity in order to reduce fading impairment; however, it is not able to mitigate neither the MAI nor the near-far effect Moshavi (1996); Verdú (1998). In this context, multiuser detection (MUD) emerged as a solution to overcome the MAI. The best performance is acquired by the optimum multiuser detection (OMUD), which is based on the log-likelihood function (LLF), but results

in a non-deterministic polynomial-time hard (NP-hard) complexity Verdú (1989). After the Verdu's revolutionary work, a great variety of suboptimal approaches have been proposed, such as (non-)linear multiuser detectors Castoldi (2002); Verdú (1998) and heuristic multiuser detectors Ergün & Hacioglu (2000); Juntti et al. (1997).

Heuristic methods have been proposed for solving the MUD problem, obtaining near-optimum performance at cost of polynomial computational complexity Abrão et al. (2009); Ergün & Hacioglu (2000). Examples of heuristic multiuser detection (HEUR-MUD) methods include: evolutionary programming (EP), specially the genetic algorithm (GA) Ciriaco et al. (2006); Ergün & Hacioglu (2000), particle swarm optimization (PSO) Khan et al. (2006); Oliveira et al. (2006); Zhao et al. (2006) and, sometimes included in this classification, the deterministic local search (LS) methods Lim & Venkatesh (2003); Oliveira et al. (2009), which has been shown very attractive performance $\times$ complexity trade-offs for low order modulation formats. High-order modulation HEUR-MUD in SISO or MIMO systems were previously addressed in Khan et al. (2006); Oliveira et al. (2008); Zhao et al. (2006). In Oliveira et al. (2008), PSO was applied to near-optimum asynchronous $16-$QAM DS/CDMA multiuser detection problem under SISO multipath channels. Previous results on literature Abrão et al. (2009); Oliveira et al. (2006) suggest that evolutionary algorithms and particle swarm optimization have similar performance, and that a simple local search heuristic optimization is enough to solve the MUD problem with low-order modulation Oliveira et al. (2009). However for high-order modulation formats, the LS-MUD does not achieve good performances due to a lack of search diversity, whereas the PSO-MUD has been shown to be more efficient for solving the optimization problem under M-QAM modulation Oliveira et al. (2008). Firstly, in this chapter the multiuser detection optimization problem is treated under a heuristic perspective. A wide analysis is carried out considering multiple access systems under BPSK, QPSK and 16-QAM modulation formats, and diversity exploration as well.

A second optimization problem treated in this chapter refers to the resources allocation in wireless multiple access networks. In order to satisfy consumers necessities while keeping companies' profits, the resource allocation issues associated to these networks must be examined, mainly spectrum and power[1] allocation schemes. Thus, many researchers have been seeking resource allocation algorithms that could be easily applied to multiple access networks with high performance guarantee, i.e. low complexity combined with high solution quality. The application of heuristic optimization to the power allocation in CDMA systems was discussed in Elkamchouchi et al. (2007); Moustafa et al. (2000). In Moustafa et al. (2000; 2001a), a genetic approach, named genetic algorithm for mobiles equilibrium (GAME), was considered in order to control two main resources in a wireless network: bit rate and corresponding transmitting power level from mobile terminals. The basic idea is that all the mobile terminals have to harmonize their rate and power according to their location, QoS, and density. However, due to the centralized nature of the power-rate allocation problem and the complexity aspects, the GAME algorithm is suitable to be implemented in the base station only, which forwards the controlling signals to the mobile terminals.

Another heuristic approach that solve efficiently the power allocation problem, while resulting in lower computational complexity than genetic schemes, involves the swarm intelligence principle. In Elkamchouchi et al. (2007), particle swarm optimization (PSO) algorithm was used to solve the power allocation problem, while in Zielinski et al. (2009)

---

[1] Power allocation procedures imply in battery autonomy improvement.

the power control scheme with PSO was associated with parallel interference cancelation multiuser detector.

On the other hand, from an analytical perspective, the classical power allocation problem in wireless networks, posed two decades ago, has been analyzed and investigated over the years and many deterministic (semi-)analytical algorithms were proposed to solve this specific problem. One of these algorithms proposed by Foschini and Miljanic Foschini & Miljanic (1993) have been considered the foundation of many well-known distributed power control algorithms (DPCA).

More recently, many researchers have proposed new algorithms to solve the resource allocation problem in wireless networks. A distributed power control algorithm for the downlink of multiclass wireless networks was proposed in Lee et al. (2005). Also, under specific scenario of interference-limited networks, a power allocation algorithm to achieve global optimality in weighted throughput maximization based on multiplicative linear fractional programming (MLFP) was proposed in Li Ping Qian (2009). Moreover, in Dai et al. (2009) the goal is to maximize the fairness between users in the uplink of CDMA systems, satisfying different QoS requirements. In Gross et al. (2010) the Verhulst mathematical model, initially designed to describe population growth of biological species with food and physical space restriction, was adapted to a single rate DS/CDMA system DPCA. The work was the first to propose a Verhulst equilibrium equation adaptation to resource allocation problems in DS/CDMA networks.

In this chapter, optimization procedures based on particle swarm intelligence are investigated in details, aiming to efficiently solve the rate allocation problem (throughput maximization) with power constraint in multiclass DS/CDMA wireless networks, which show different QoS requirements, related to different user classes, making the resource allocation optimization procedure a more challenging task.

The chapter is organized in the following manner: in Section 2 the multiuser detection problem is treated under a guided search perspective, while in Section 3 a second class of optimization problem, namely the power and rate allocation problem in multi-class QoS multiple access networks is analyzed under the same heuristic optimization principle. In each multiple access network optimization context, after system model description, figures of merit are presented and a suitable swarm algorithm version is developed, with emphasis in the optimization of PSO' input parameters. Afterward, extensive numerical results for both problems are discussed for realistic networks operation scenarios. Finally, the main conclusions are offered in Section 4.

2. Multiuser detection problem

This section focuses on the DS/CDMA multiuser problem. A single-cell asynchronous multiple access DS/CDMA system model is described for Rayleigh channels, considering different modulation schemes, such as binary/quadrature phase shift keying (BPSK/QPSK) and 16-quadrature amplitude modulation (16-QAM), and single or multiple antennas at the base station receiver. After describing the conventional detection approach with a maximum ratio combining (MRC) rule, the OMuD and the PSO-MuD are described. The model is generic enough to allow describing additive white Gaussian noise (AWGN) and Rayleigh flat channels, other modulation formats and single-antenna receiver.

2.1 DS/CDMA

The base-band transmitted signal of the kth user is described as Proakis (1989)

$$s_k(t) = \sqrt{\frac{\mathcal{E}_k}{T}} \sum_{i=-\infty}^{\infty} d_k^{(i)} g_k(t - iT), \tag{1}$$

where $\mathcal{E}_k$ is the symbol energy, and T is the symbol duration. Each symbol $d_k^{(i)}$, $k = 1, \ldots, K$ is taken independently and with equal probability from a complex alphabet set $\mathcal{A}$ of cardinality $M = 2^m$ in a squared constellation, i.e., $d_k^{(i)} \in \mathcal{A} \subset \mathbb{C}$, where $\mathbb{C}$ is the set of complex numbers. Fig. 1 shows the modulation formats considered, while Fig. 2 sketches the K base-band DS/CDMA transmitters.
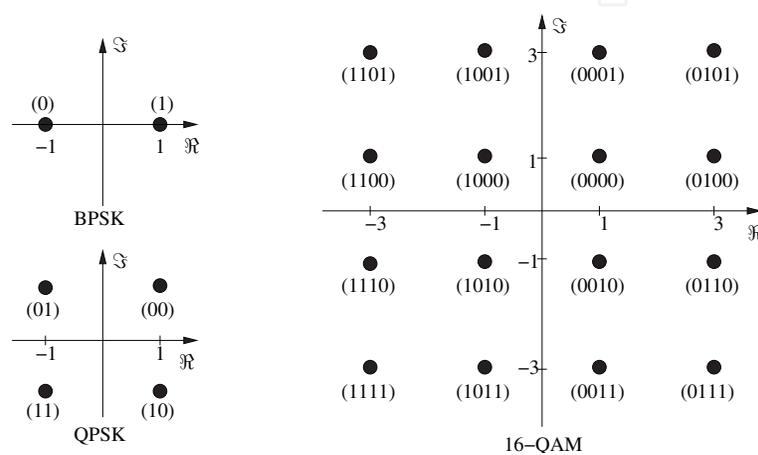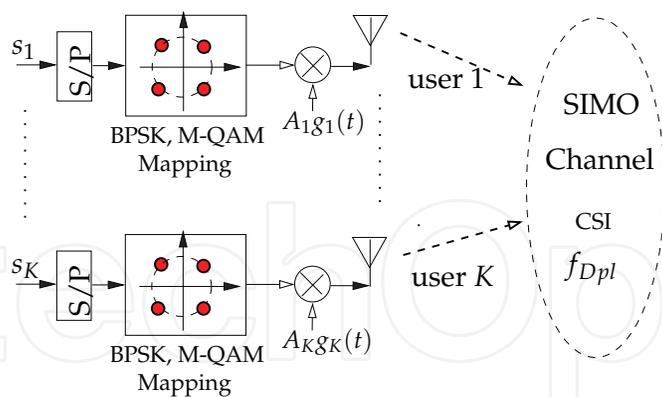

Fig. 1. Three modulation formats with Gray mapping.

Fig. 2. Uplink base-band DS/CDMA transmission model with K users.

The normalized spreading sequence for the k-th user is given by

$$g_k(t) = \frac{1}{\sqrt{N}} \sum_{n=0}^{N-1} a_k(n) p(t - nT_c), \qquad 0 \leq t \leq T, \tag{2}$$

where $a_k(n)$ is a random sequence with N chips assuming the values $\{\pm 1\}$, $p(t)$ is the pulse shaping, assumed rectangular with unitary amplitude and duration T_c, with T_c being the chip interval. The processing gain is given by $N = T/T_c$.

The equivalent base-band received signal at qth receive antenna, $q = 1, 2, \ldots, Q$, containing I symbols for each user in multipath fading channel can be expressed by

$$r_q(t) = \sum_{i=0}^{I-1} \sum_{k=1}^{K} \sum_{\ell=1}^{L} A_k d_k^{(i)} g_k(t - nT - \tau_{q,k,\ell}) h_{q,k,\ell}^{(i)} e^{j\varphi_{q,k,\ell}} + \eta_q(t), \tag{3}$$

with $A_k = \sqrt{\frac{\mathcal{E}_k}{T}}$, L being the number of channel paths, admitted equal for all K users, $\tau_{q,k,\ell}$ is the total delay[2] for the signal of the kth user, ℓth path at qth receive antenna, $e^{j\varphi_{q,k,\ell}}$ is the respective received phase carrier; $\eta_q(t)$ is the additive white Gaussian noise with bilateral power spectral density equal to $N_0/2$, and $h_{q,k,\ell}^{(i)}$ is the complex channel coefficient for the ith symbol, defined as

$$h_{q,k,\ell}^{(i)} = \gamma_{q,k,\ell}^{(i)} e^{j\theta_{q,k,\ell}^{(i)}}, \tag{4}$$

where the channel gain (modulo) $\gamma_{q,k,\ell}^{(i)}$ is characterized by a Rayleigh distribution and the phase $\theta_{q,k,\ell}^{(i)}$ by the uniform distribution $\mathcal{U}[0, 2\pi]$.

Generally, a slow and frequency selective channel[3] is assumed. The expression in (3) is quite general and includes some special and important cases: if $Q = 1$, a SISO system is obtained; if $L = 1$, the channel becomes non-selective (flat) Rayleigh; if $h_{q,k,\ell}^{(i)} = 1$, it results in the AWGN channel. Moreover, if $|\tau_{q,k,\ell}| \leq \epsilon_\tau$, with $\epsilon_\tau \in [0; 3T_c]$, a quasi-synchronous DS/CDMA system can be characterized.

At the base station, the received signal is submitted to a matched filter bank (CD), with $D \leq L$ branches (fingers) per antenna of each user. When $D \geq 1$, CD is known as Rake receiver. Assuming perfect phase estimation (carrier phase), after despreading the resultant signal is given by

$$\begin{aligned} y_{q,k,\ell}^{(i)} &= \frac{1}{T} \int_{nT}^{(i+1)T} r_q(t) g_k(t - \tau_{q,k,\ell}) dt \\ &= A_k h_{q,k,\ell}^{(i)} d_k^{(i)} + SI_{q,k,\ell}^{(i)} + I_{q,k,\ell}^{(i)} + \widetilde{\eta}_{q,k,\ell}^{(i)}. \end{aligned} \tag{5}$$

The first term is the signal of interest, the second corresponds to the self-interference (SI), the third to the multiple-access interference (MAI) and the last one corresponds to the filtered AWGN.

Considering a maximal ratio combining (MRC) rule with diversity order equal to DQ for each user, the $M-$level complex decision variable is given by

$$\zeta_k^{(i)} = \sum_{q=1}^{Q} \sum_{\ell=1}^{D} y_{q,k,\ell}^{(i)} \cdot w_{q,k,\ell}^{(i)}, \quad k = 1, \ldots, K \tag{6}$$

where the MRC weights $w_{q,k,\ell}^{(i)} = \widehat{\gamma}_{q,k,\ell}^{(i)} e^{-j\widehat{\theta}_{q,k,\ell}^{(i)}}$, with $\widehat{\gamma}_{q,k,l}^{(i)}$ and $\widehat{\theta}_{q,k,\ell}^{(i)}$ been a channel amplitude and phase estimation, respectively.

---

[2] Considering the asynchronism among the users and random delays for different paths.

[3] Slow channel: channel coefficients were admitted constant along the symbol period T; and frequency selective condition is hold: $\frac{1}{T_c} >> (\Delta B)_c$, the coherence bandwidth of the channel.

After that, at each symbol interval, decisions are made on the in-phase and quadrature components[4] of $\zeta_k^{(i)}$ by scaling it into the constellation limits obtaining $\xi_k^{(i)}$, and choosing the complex symbol with minimum Euclidean distance regarding the scaled decision variable. Alternatively, this procedure can be replaced by separate $\sqrt{M}-$level quantizers qtz acting on the in-phase and quadrature terms separately, such that

$$\widehat{d}_k^{(i),\text{CD}} = \underset{\mathcal{A}_{\text{real}}}{\text{qtz}} \left(\Re \left\{ \xi_k^{(i)} \right\} \right) + j \underset{\mathcal{A}_{\text{imag}}}{\text{qtz}} \left(\Im \left\{ \xi_k^{(i)} \right\} \right), \tag{7}$$

for $k = 1, \ldots, K$, been $\mathcal{A}_{\text{real}}$ and $\mathcal{A}_{\text{imag}}$ the real and imaginary value sets, respectively, from the complex alphabet set $\mathcal{A}$, and $\Re\{\cdot\}$ and $\Im\{\cdot\}$ representing the real and imaginary operators, respectively. Fig. 3 illustrates the general system structure.
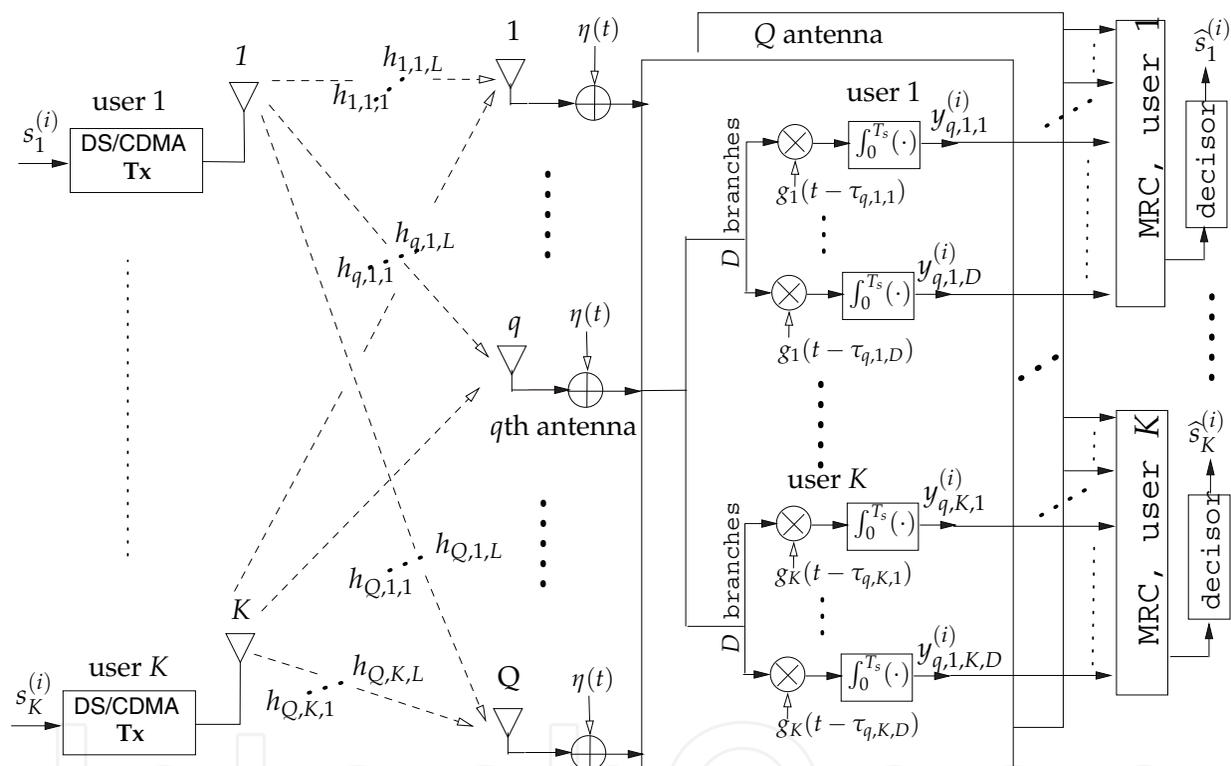

Fig. 3. Uplink base-band DS/CDMA system model: K users transmitters, SIMO channel and Conventional (Rake) receiver with Q multiple receive antennas.

2.2 Optimum detection

The OMuD estimates the symbols for all K users by choosing the symbol combination associated with the minimal distance metric among all possible symbol combinations in the $M = 2^m$ constellation points Verdú (1998).

In the asynchronous multipath channel scenario considered in this chapter, the one-shot asynchronous channel approach is adopted, where a configuration with K asynchronous users, I symbols and D branches is equivalent to a synchronous scenario with KID virtual users.

---

[4] Note that, for BPSK, only the in-phase term is presented.

Furthermore, in order to avoid handling complex-valued variables in high-order squared modulation formats, henceforward the alphabet set is re-arranged as $\mathcal{A}_{\text{real}} = \mathcal{A}_{\text{imag}} = \mathcal{Y} \subset \mathbb{Z}$ of cardinality $\sqrt{M}$, e.g., $16-$QAM ($m = 4$): $d_k^{(i)} \in \mathcal{Y} = \{\pm 1, \pm 3\}$.

The OMUD is based on the maximum likelihood criterion that chooses the vector of symbols $\underline{\mathbf{d}}_p$, formally defined in (12), which maximizes the metric

$$\underline{\mathbf{d}}^{\text{opt}} = \arg \max_{\underline{\mathbf{d}}_p \in \mathcal{Y}^{2KID}} \left\{ \Omega\left(\underline{\mathbf{d}}_p\right) \right\}, \tag{8}$$

where, in a SIMO channel, the single-objective function is generally written as a combination of the LLFs from all receive antennas, given by

$$\Omega\left(\underline{\mathbf{d}}_p\right) = \sum_{q=1}^{Q} \Omega_q\left(\underline{\mathbf{d}}_p\right). \tag{9}$$

In a more general case considered herein, namely K asynchronous users in a SIMO multipath Rayleigh channel with diversity $D \leq L$, the LLF can be defined as a decoupled optimization problem with only real-valued variables, such that

$$\Omega_q(\underline{\mathbf{d}}_p) = 2\underline{\mathbf{d}}_p^\top \mathbf{W}_q^\top \underline{\mathbf{y}}_q - \underline{\mathbf{d}}_p^\top \mathbf{W}_q \underline{\mathbf{R}} \mathbf{W}_q^\top \underline{\mathbf{d}}_p, \tag{10}$$

with definitions

$$\underline{\mathbf{d}}_p \triangleq \begin{bmatrix} \Re\{\mathbf{d}_p\} \\ \Im\{\mathbf{d}_p\} \end{bmatrix}; \quad \mathbf{W}_q \triangleq \begin{bmatrix} \Re\{\mathbf{AH}\} & -\Im\{\mathbf{AH}\} \\ \Im\{\mathbf{AH}\} & \Re\{\mathbf{AH}\} \end{bmatrix}; \quad \underline{\mathbf{y}}_q \triangleq \begin{bmatrix} \Re\{\mathbf{y}_q\} \\ \Im\{\mathbf{y}_q\} \end{bmatrix}; \quad \underline{\mathbf{R}} \triangleq \begin{bmatrix} \mathbf{R} & 0 \\ 0 & \mathbf{R} \end{bmatrix}, \tag{11}$$

where $\underline{\mathbf{y}}_q \in \mathbb{R}^{2KID \times 1}$, $\mathbf{W}_q \in \mathbb{R}^{2KID \times 2KID}$, $\underline{\mathbf{d}}_p \in \mathcal{Y}^{2KID \times 1}$, $\underline{\mathbf{R}} \in \mathbb{R}^{2KID \times 2KID}$. The vector $\mathbf{d}_p \in \mathcal{Y}^{KID \times 1}$ in Eq. (11) is defined as

$$\mathbf{d}_p = [\underbrace{(d_1^{(1)} \cdots d_1^{(1)}}_{D \text{ times}}) \cdots \underbrace{(d_K^{(1)} \cdots d_K^{(1)}}_{D \text{ times}}) \cdots \underbrace{(d_1^{(I)} \cdots d_1^{(I)}}_{D \text{ times}}) \cdots \underbrace{(d_K^{(I)} \cdots d_K^{(I)}}_{D \text{ times}})]^\top. \tag{12}$$

In addition, the $\mathbf{y}_q \in \mathbb{C}^{KID \times 1}$ is the despread signal in Eq. (6) for a given q, in a vector notation, described as

$$\underline{\mathbf{y}}_q = \left[(y_{q,1,1}^{(1)} \cdots y_{q,1,D}^{(1)}) \cdots (y_{q,K,1}^{(1)} \cdots y_{q,K,D}^{(1)}) \cdots (y_{q,1,1}^{(I)} \cdots y_{q,1,D}^{(I)}) \cdots (y_{q,K,1}^{(I)} \cdots y_{q,K,D}^{(I)})\right] \tag{13}$$

Matrices $\mathbf{H}$ and $\mathbf{A}$ are the coefficients and amplitudes diagonal matrices, respectively, and $\mathbf{R}$ represents the block-tridiagonal, block-Toeplitz cross-correlation matrix, composed by the sub-matrices $\mathbf{R}[1]$ and $\mathbf{R}[0]$, such that Verdú (1998)

$$\mathbf{R} = \begin{bmatrix} \mathbf{R}[0] & \mathbf{R}[1]^\top & 0 & \dots & 0 & 0 \\ \mathbf{R}[1] & \mathbf{R}[0] & \mathbf{R}[1]^\top & \dots & 0 & 0 \\ 0 & \mathbf{R}[1] & \mathbf{R}[0] & \dots & 0 & 0 \\ \dots & \dots & \dots & \dots & \dots & \dots \\ 0 & 0 & 0 & \dots & \mathbf{R}[1] & \mathbf{R}[0] \end{bmatrix}, \tag{14}$$

with $\mathbf{R}[0]$ and $\mathbf{R}[1]$ being KD matrices with elements

$$\underline{\rho_{a,b}}[0] = \begin{cases} 1, & \text{if } (k=u) \text{ and } (\ell = l) \\ \rho^q_{k,\ell,u,l}, & \text{if } (k<u) \text{ or } (k=u, \ell < l) \\ \rho^q_{u,l,k,\ell}, & \text{if } (k>u) \text{ or } (k=u, \ell > l), \end{cases}$$

$$\underline{\rho_{a,b}}[1] = \begin{cases} 0, & \text{if } k \geq u \\ \rho^q_{u,l,k,\ell}, & \text{if } k < u \end{cases}' \tag{15}$$

where $a = (k-1)D + \ell$, $b = (u-1)D + l$ and $k, u = 1, 2, \ldots, K$; $\ell, l = 1, 2, \ldots, D$; the cross-correlation element between the kth user, ℓth path and uth user, dth path, at qth receive antenna is defined by:

$$\rho^q_{k,\ell,u,d} = \frac{1}{T} \int_0^T g_k(t - \tau_{q,k,\ell}) g_u(t - \tau_{q,u,d}) dt. \tag{16}$$

The evaluation in (8) can be extended along the whole message, where all symbols of the transmitted vector for all K users are jointly detected, namely vector maximum-likelihood (ML) approach, or the decisions can be taken considering the optimal single symbol detection of all K multiuser signals (symbol ML approach). In the synchronous case, the symbol ML approach with $I = 1$ is considered, whereas in the asynchronous case the vector ML approach is adopted with $I = 7$ (I must be, at least, equal to three ($I \geq 3$)).

The vector $\underline{\mathbf{d}}_p$ in (11) belongs to a discrete set with size depending on M, K, I and D. Hence, the optimization problem posed by (8) can be solved directly using a $m-$dimensional ($m = \log_2 M$) search method. Therefore, the associated combinatorial problem strictly requires an exhaustive search in $\mathcal{A}^{KID}$ possibilities of $\mathbf{d}$, or equivalently an exhaustive search in $\mathcal{Y}^{2KID}$ possibilities of $\underline{\mathbf{d}}_p$ for the decoupled optimization problem with only real-valued variables. As a result, the maximum likelihood detector has a complexity that increases exponentially with the modulation order, number of users, symbols and branches, becoming prohibitive even for moderate product values $mKID$, i.e., even for a BPSK modulation format, medium system loading (K/N), small number of symbols I and realistic values for the D Rake fingers (around 4 to 6).

2.3 Discrete swarm optimization algorithm

A discrete or, in several cases, binary PSO Kennedy & Eberhart (1997) is considered in this chapter. Such scheme is suitable to deal with digital information detection/decoding. Hence, binary PSO is adopted herein. The particle selection for evolving is based on the highest fitness values obtained through (10) and (9).

Accordingly, each candidate-vector defined like $\mathbf{d}_i$ has its binary representation, $\mathbf{b}_p[t]$, of size mKI, used for the velocity calculation, and the pth PSO particle position at instant (iteration) t is represented by the $mKI \times 1$ binary vector

$$\mathbf{b}_p[t] = [\mathbf{b}_p^1 \, \mathbf{b}_p^2 \, \cdots \, \mathbf{b}_p^r \, \cdots \, \mathbf{b}_p^{KI}]; \qquad \text{with} \quad \mathbf{b}_p^r = \left[b_{p,1}^r \cdots b_{p,v}^r \cdots b_{p,m}^r \right]; \quad b_{p,v}^r \in \{0, 1\}, \tag{17}$$

where each binary vector $\mathbf{b}_p^r$ is associated with one $d_k^{(i)}$ symbol in Eq. (12). Each particle has a velocity, which is calculated and updated according to

$$\mathbf{v}_p[t+1] = \omega \cdot \mathbf{v}_p[t] + \phi_1 \cdot \mathbf{U}_{p_1}[t](\mathbf{b}_p^{\text{best}}[t] - \mathbf{b}_p[t]) + \phi_2 \cdot \mathbf{U}_{p_2}[t](\mathbf{b}_g^{\text{best}}[t] - \mathbf{b}_p[t]), \tag{18}$$

where ω is the inertial weight; $\mathbf{U}_{p_1}[t]$ and $\mathbf{U}_{p_2}[t]$ are diagonal matrices with dimension mKI, whose elements are random variables with uniform distribution $\mathcal{U} \in [0,1]$; $\mathbf{b}_g^{\text{best}}[t]$ and $\mathbf{b}_p^{\text{best}}[t]$ are the best global position and the best local positions found until the tth iteration, respectively; ϕ_1 and ϕ_2 are weight factors (acceleration coefficients) regarding the best individual and the best global positions influences in the velocity update, respectively.

For MuD optimization with binary representation, each element of $\mathbf{b}_p[t]$ in (18) just assumes "0" or "1" values. Hence, a discrete mode for the position choice is carried out inserting a probabilistic decision step based on threshold, depending on the velocity. Several functions have this characteristic, such as the sigmoid function Kennedy & Eberhart (1997)

$$S(v_{p,v}^r[t]) = \frac{1}{1 + e^{-v_{p,v}^r[t]}}, \tag{19}$$

where $v_{p,v}^r[t]$ is the rth element of the pth particle velocity vector, $\mathbf{v}_p^r = \left[v_{p,1}^r \cdots v_{p,v}^r \cdots v_{p,m}^r \right]$, and the selection of the future particle position is obtained through the statement

$$\begin{aligned} \text{if} \quad & u_{p,v}^r[t] < S(v_{p,v}^r[t]), \quad && b_{p,v}^r[t+1] = 1; \\ & \text{otherwise}, \quad && b_{p,v}^r[t+1] = 0, \end{aligned} \tag{20}$$

where $b_{p,v}^r[t]$ is an element of $\mathbf{b}_p[t]$ (see Eq. (17)), and $u_{p,v}^r[t]$ is a random variable with uniform distribution $\mathcal{U} \in [0,1]$.

After obtaining a new particle position $\mathbf{b}_p[t+1]$, it is mapped back into its correspondent symbol vector $\mathbf{d}_p[t+1]$, and further in the real form $\underline{\mathbf{d}}_p[t+1]$, for the evaluation of the objective function in (9).

In order to obtain further diversity for the search universe, the $V_{\max}$ factor is added to the PSO model, Eq. (18), being responsible for limiting the velocity in the range $[\pm V_{\max}]$. The insertion of this factor in the velocity calculation enables the algorithm to escape from possible local optima. The likelihood of a bit change increases as the particle velocity crosses the limits established by $[\pm V_{\max}]$, as shown in Table 1.

Table 1. Minimum bit change probability as a function of $V_{\max}$.

$V_{\max}$	1	2	3	4	5
$1 - S(V_{\max})$	0.269	0.119	0.047	0.018	0.007

Population size $\mathcal{P}$ is typically in the range of 10 to 40 Eberhart & Shi (2001). However, based on Oliveira et al. (2006), it is set to

$$\mathcal{P} = 10 \left\lfloor 0.3454 \left(\sqrt{\pi(mKI - 1)} + 2 \right) \right\rfloor. \tag{21}$$

Algorithm 1 describes the pseudo-code for the PSO implementation.

2.4 Parameters optimization for PSO-MuD

The PSO-MuD parameters optimization is carried out using Monte-Carlo simulation Jeruchim et al. (1992). Such an optimization is directly related to the complexity $\times$ performance trade-off of the algorithm. A wide analysis with BPSK, QPSK and 16-QAM modulation schemes, and diversity exploration is carried out.

Algorithm 1 SOO Discrete PSO Algorithm for the MUD Problem

Input: $\mathbf{d}^{CD}, \mathcal{P}, G, \omega, \phi_1, \phi_2, V_{max}$;   **Output:** $\mathbf{d}^{PSO}$

begin
1.   initialize first population: $\mathtt{t} = 0$;
          $\mathbf{B}[0] = \mathbf{b}^{CD} \cup \widetilde{\mathbf{B}}$, where $\widetilde{\mathbf{B}}$ contains $(\mathcal{P}-1)$ particles randomly
        generated;
          $\mathbf{b}_p^{best}[0] = \mathbf{b}_p[0]$ and $\mathbf{b}_g^{best}[0] = \mathbf{b}^{CD}$;
          $\mathbf{v}_p[0] = \mathbf{0}$: null initial velocity;
2.   while $\mathtt{t} \leq G$
          a. calculate $\Omega(\underline{\mathbf{d}}_p[\mathtt{t}]), \forall \mathbf{b}_p[\mathtt{t}] \in \mathbf{B}[\mathtt{t}]$ using (9);
          b. update velocity $\mathbf{v}_p[\mathtt{t}]$, $p = 1, \ldots, \mathcal{P}$, through (18);
          c. update best positions:
                for $p = 1, \ldots, \mathcal{P}$
                    if $\Omega(\underline{\mathbf{d}}_p[\mathtt{t}]) > \Omega(\underline{\mathbf{d}}_p^{best}[\mathtt{t}])$, $\mathbf{b}_p^{best}[\mathtt{t}+1] \leftarrow \mathbf{b}_p[\mathtt{t}]$
                    else $\mathbf{b}_p^{best}[\mathtt{t}+1] \leftarrow \mathbf{b}_p^{best}[\mathtt{t}]$
                end
                if $\exists\, \mathbf{b}_p[\mathtt{t}]$ such that $\left[\Omega(\underline{\mathbf{d}}_p[\mathtt{t}]) > \Omega(\underline{\mathbf{d}}_g^{best}[\mathtt{t}])\right] \wedge$
                                                    $\left[\Omega(\underline{\mathbf{d}}_p[\mathtt{t}]) \geq \Omega(\underline{\mathbf{d}}_j[\mathtt{t}]), j \neq p\right]$,
                    $\mathbf{b}_g^{best}[\mathtt{t}+1] \leftarrow \mathbf{b}_p[\mathtt{t}]$
                    else $\mathbf{b}_g^{best}[\mathtt{t}+1] \leftarrow \mathbf{b}_g^{best}[\mathtt{t}]$
          d. Evolve to a new swarm population $\mathbf{B}[\mathtt{t}+1]$, using (20);
          e. set $\mathtt{t} = \mathtt{t}+1$.
        end
3. $\mathbf{b}^{PSO} = \mathbf{b}_g^{best}[G]$; $\mathbf{b}^{PSO} \xrightarrow{\text{map}} \mathbf{d}^{PSO}$.
end
$- -$
$\mathbf{d}^{CD}$: CD output.
$\mathcal{P}$: Population size.
G: number of swarm iterations.
For each $\underline{\mathbf{d}}_p[\mathtt{t}]$ there is a $\mathbf{b}_p[\mathtt{t}]$ associated.

A first analysis of the PSO parameters gives raise to the following behaviors: ω is responsible for creating an inertia of the particles, inducing them to keep the movement towards the last directions of their velocities; ϕ_1 aims to guide the particles to each individual best position, inserting diversification in the search; ϕ_2 leads all particles towards the best global position, hence intensifying the search and reducing the convergence time; V_{max} inserts perturbation limits in the movement of the particles, allowing more or less diversification in the algorithm. The optimization process for the initial velocity of the particles achieves similar results for three different conditions: null, random and CD output as initial velocity. Hence, it is adopted here, for simplicity, null initial velocity, i.e., $\mathbf{v}[0] = \mathbf{0}$.

In Oliveira et al. (2006), the best performance × complexity trade-off for BPSK PSO-MUD algorithm was obtained setting $V_{max} = 4$. Herein, simulations carried out varying V_{max} for different modulations and diversity exploration accomplish this value as a good alternative. This optimization process is quite similar for systems with QPSK and 16-QAM modulation formats.

2.4.1 ω optimization

It is worth noting that a relatively larger value for ω is helpful for global optimum, and lesser influenced by the best global and local positions, while a relatively smaller value for ω is helpful for course convergence, i.e., smaller inertial weight encourages the local exploration Eberhart & Shi (2001); Shi & Eberhart (1998) as the particles are more attracted towards $\mathbf{b}_p^{best}[t]$ and $\mathbf{b}_g^{best}[t]$.

Fig. 4 shows the convergence of the PSO scheme for different values of ω considering BPSK modulation and flat channel. It is evident that the best performance $\times$ complexity trade-off is accomplished with $\omega = 1$.
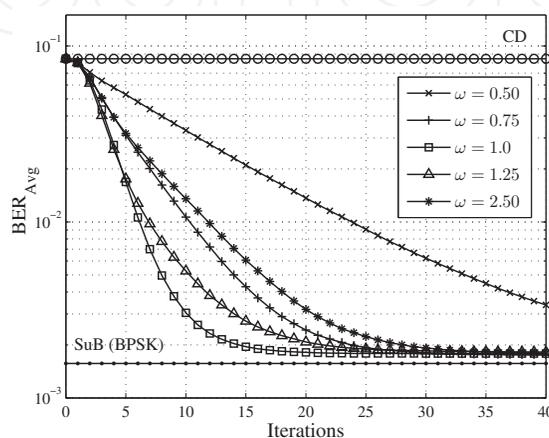

Fig. 4. ω optimization under Rayleigh flat channels with BPSK modulation, $E_b/N_0 = 22$ dB, $K = 15$, $\phi_1 = 2$, $\phi_2 = 10$ and $V_{max} = 4$.

Many research' papers have been reported new PSO procedures and strategies in order to improve its performance and reduce its complexity. For instance, in Chatterjee & Siarry (2006) the authors have been discussed adaptive nonlinear inertia weight in order to improve PSO convergence. However, the current analysis indicates that no further specialized strategy is necessary, since the conventional PSO works well to solve the MuD DS/CDMA problem in several practical scenarios.

The optimization of the inertial weight, ω, achieves analogous results for QPSK and 16-QAM modulation schemes, where $\omega = 1$ also achieves the best performance $\times$ complexity trade-off (results not shown). In the next Subsection, a special attention is given for ϕ_1 and ϕ_2 input parameter optimization, since their values impact deeply in the PSO performance, also varying for each order modulation.

2.4.2 ϕ_1 and ϕ_2 optimization

For BPSK modulation and Rayleigh flat channels, the performance improvement expected by ϕ_1 increment is not evident, and its value can be reduced without performance losses, as can be seen in Fig. 5. Therefore, a good choice seems to be $\phi_1 = 2$, achieving a reasonable convergence rate.

Fig. 6.(a) illustrates different convergence performances achieved with $\phi_1 = 2$ and $\phi_2 \in [1; 15]$ for medium system loading and medium-high E_b/N_0. Even for high system loading, the PSO performance is quite similar for different values of ϕ_2, as observed in Fig. 6.(b). Hence, considering the performance $\times$ complexity trade-off, a reasonable choice for ϕ_2 under Rayleigh flat channels is $\phi_2 = 10$.
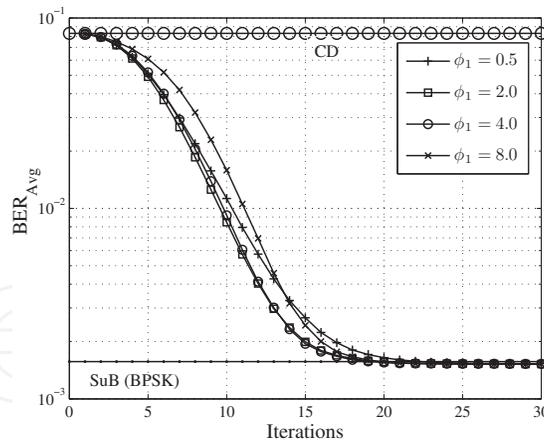
Fig. 5. ϕ_1 optimization in Rayleigh flat channels with BPSK modulation, $E_b/N_0 = 22$ dB, $K = 15$, $\phi_2 = 10$ (fixed), $V_{\max} = 4$, and $\omega = 1$.
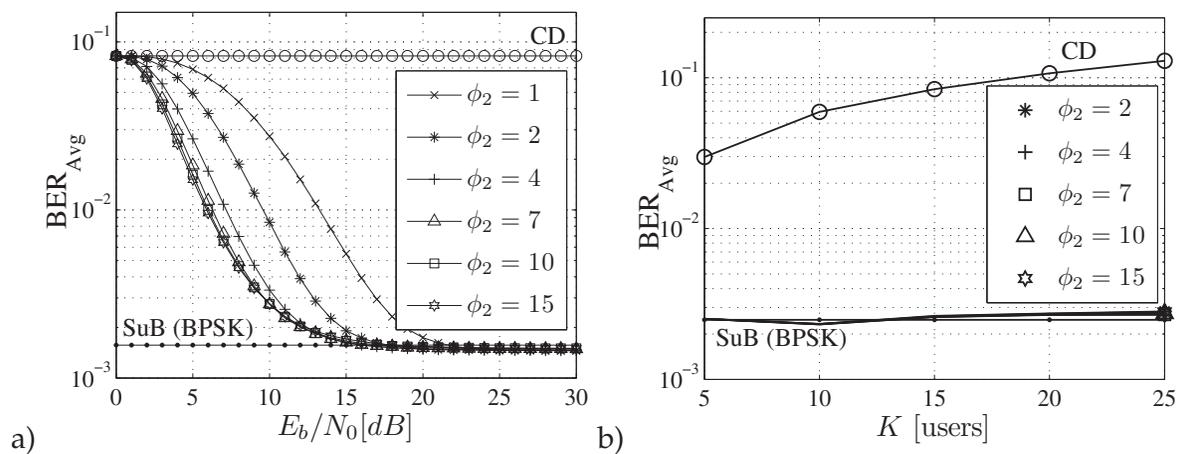

Fig. 6. ϕ_2 optimization in Rayleigh flat channels with BPSK modulation, $V_{\max} = 4$, $\omega = 1$, and $\phi_1 = 2$ (fixed); a) convergence performance with $E_b/N_0 = 22$ dB and $K = 15$; b) average BER $\times$ K with $E_b/N_0 = 20$ dB, $G = 30$ iterations.

Different results from BPSK are achieved when a QPSK modulation scheme is adopted. Note in Fig. 7 that low values of ϕ_2 and high values ϕ_1 delay the convergence, the inverse results in lack of diversity. Hence, the best performance $\times$ complexity is achieved with $\phi_1 = \phi_2 = 4$.

Under 16-QAM modulation, the PSO-MUD requires more intensification, once the search becomes more complex due to each symbol maps to 4 bits. Fig. 8 shows the convergence curves for different values of ϕ_1 and ϕ_2, where it is clear that the performance gap is more evident with an increasing number of users and E_b/N_0. Analyzing this result, the chosen values are $\phi_1 = 6$ and $\phi_2 = 1$.

The best range for the acceleration coefficients under resolvable multipath channels ($L \geq 2$) for MuD SISO DS/CDMA problem seems $\phi_1 = 2$ and $\phi_2 \in [12; 15]$, as indicated by the simulation results shown in Fig. 9. For medium system loading and SNR, Fig. 9 indicates that the best values for acceleration coefficients are $\phi_1 = 2$ and $\phi_2 = 15$, allowing the combination of fast convergence and near-optimum performance achievement.

The optimized input parameters for PSO-MUD vary regarding the system and channel scenario conditions. Monte-Carlo simulations exhibited in Section 2.5 adopt the values
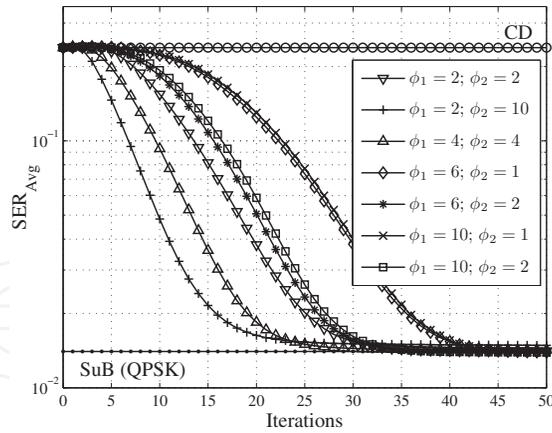
Fig. 7. ϕ_1 and ϕ_2 optimization under flat Rayleigh channels for QPSK modulation, $E_b/N_0 = 22$ dB, $K = 15$, $\omega = 1$ and $V_{\max} = 4$.
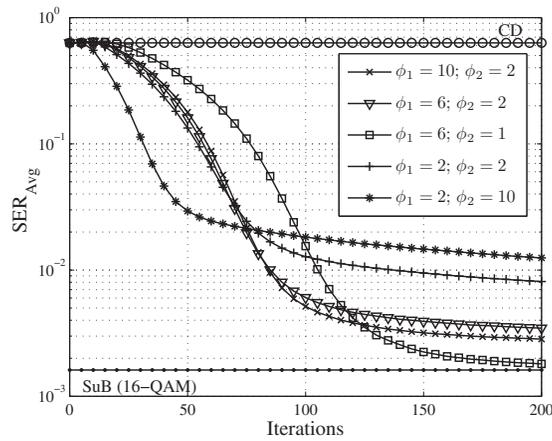

Fig. 8. ϕ_1 and ϕ_2 optimization under flat Rayleigh channels for 16-QAM modulation, $E_b/N_0 = 30$ dB, $K = 15$, $\omega = 1$ and $V_{\max} = 4$.
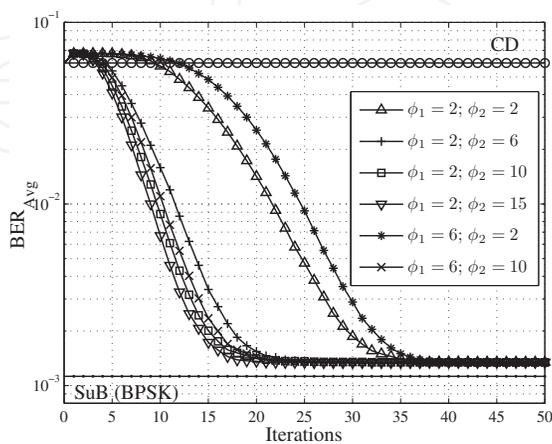

Fig. 9. ϕ_1 and ϕ_2 optimization under Rayleigh channels with path diversity ($L = D = 2$) for BPSK modulation, $E_b/N_0 = 22$ dB, $K = 15$, $\omega = 1$, $V_{\max} = 4$.

Channel & Modulation	$\mathcal{L}$ range	ω	ϕ_1	ϕ_2	$V_{\max}$
Flat Rayleigh BPSK	[0.16; 1.00]	1	2	10	4
Flat Rayleigh QPSK	[0.16; 1.00]	1	4	4	4
Flat Rayleigh 16-QAM	[0.03; 0.50]	1	6	1	4
Diversity Rayleigh BPSK	[0.03; 0.50]	1	2	15	4

Table 2. Optimized parameters for asynchronous PSO-MuD.

presented in Table 2 as the optimized input PSO parameters for the MuD problem. Loading system $\mathcal{L}$ range indicates the boundaries for $\frac{K}{N}$ which the input PSO parameters optimization was carried out. For system operation characterized by spatial diversity ($Q > 1$ receive antennas), the PSO-MuD behaviour, in terms of convergence speed and quality of solution, is very similar to that presented under multipath diversity.

2.5 Numerical results with optimized parameters for MuD problem

Numerical performance results are obtained using Monte-Carlo simulations, with optimized PSO parameters for different loading, E_b/N_0, near-far effect, modulation, diversity exploitation and errors in the channel coefficients estimation. The results obtained are compared with theoretical single-user bound (SuB), according to Appendix A, since the OMuD computational complexity results prohibitive. The adopted PSO-MuD parameters, as well as system and channel conditions employed in Monte-Carlo simulations are summarized in Table 3.

Parameter	Adopted Values
DS/CDMA System	
# Rx antennas	$Q = 1, 2, 3$
Spreading Sequences	Random, $N = 31$
modulation	BPSK, QPSK and $16-$QAM
# mobile users	$K \in [5; 31]$
Received SNR	$E_b/N_0 \in [0; 30]$ dB
PSO-MuD Parameters	
Population size, $\mathcal{P}$	Eq. (21)
acceleration coefficients	$\phi_1 \in [2; 6]$; $\phi_2 \in [1; 10]$
inertia weight	$\omega = 1$
Maximal velocity	$V_{\max} = 4$
Rayleigh Channel	
Channel state info. (CSI)	perfectly known at Rx
	coefficient error estimates
Number of paths	$L = 1, 2, 3$

Table 3. System, channel and PSO-MuD parameters for fading channels performance analysis.

Fig. 10 presents the performance as a function of received E_b/N_0 for two different near-far ratio scenarios under flat Rayleigh channel. Fig. 10.(a) was obtained for perfect power control, whereas Fig. 10.(b) was generated considering half users with $NFR = +6$ dB. Here, the BER_{Avg} performance is calculated only for the weaker users. Note the performance of the PSO-MuD is almost constant despite of the $NFR = +6$ dB for half of the users, illustrating the robustness of the PSO-MuD against unbalanced powers in flat fading channels.

Regarding channel diversity, two assumptions are considered when there are more than one antenna at receiver (Spatial Diversity): first, the average received power is equal for
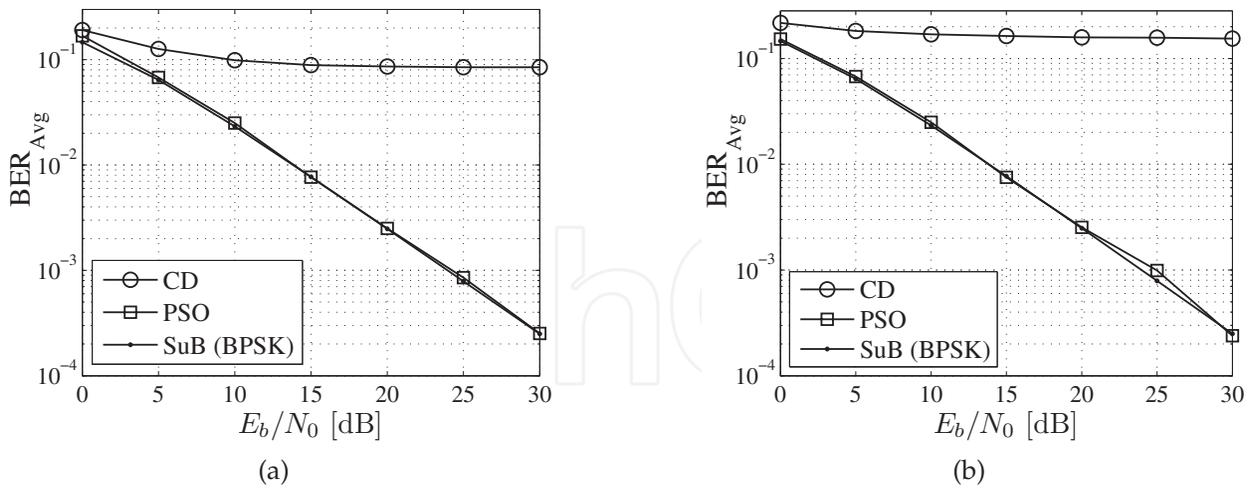
Fig. 10. Average $\text{BER}_{\text{Avg}} \times E_b/N_0$ for flat Rayleigh channel with $K = 15$: (a) perfect power control; (b) $NFR = +6$ dB for 7 users. In scenario (b), the performance is calculated only for the weaker users.

all antennas; and second, the SNR at the receiver input is defined as the received SNR per antenna. Therefore, there is a power gain of 3 dB when adopted $Q = 2$, 6 dB with $Q = 3$, and so on. The effect of increasing the number of receive antennas in the convergence curves is shown in Fig. 11, where PSO-MUD works on systems with $Q = 1$, 2 and 3 antennas. A delay in the PSO-MUD convergence is observed when more antennas are added to the receiver, caused by the larger gap that it has to surpass. Furthermore, PSO-MUD achieves the SuB performance for all the three cases.

The exploitation of the path diversity also improves the system capacity. Fig. 11 shows the BER_{Avg} convergence of PSO-MUD for different of paths, $L = 1$, 2 and 3, when the detector explores fully the path diversity, i.e., the number of fingers of conventional detector is equal the number of copies of signal received, $D = L$. The power delay profile considered is exponential, with mean paths energy as shown in Table 4 Proakis (1989). It is worth mentioning that the mean received energy is equal for the three conditions, i.e., the resultant improvement with increasing number of paths is due the diversity gain only.

Param.	PD-1	PD-2		PD-3		
Path, ℓ	1	1	2	1	2	3
τ_ℓ	0	0	T_c	0	T_c	$2T_c$
$\mathbb{E}[\gamma_\ell^2]$	1.0000	0.8320	0.1680	0.8047	0.1625	0.0328

Table 4. Three power-delay profiles for different Rayleigh fading channels used in Monte-Carlo simulations.

Note there is a performance gain with the exploration of such diversity, verified in both the Rake receiver and PSO-MUD. The PSO-MUD performance is close to SuB in all cases, exhibiting its capability of exploring path diversity and dealing with SI as well. In addition, the convergence aspects are kept for all conditions.

The PSO-MUD single-objective function, Eq. (9), takes into account the channel coefficient estimation of each user, and imperfect channel estimation degrades its performance. In order to raise a quantitative characterization of such aspect, the PSO-MUD is evaluate under channel

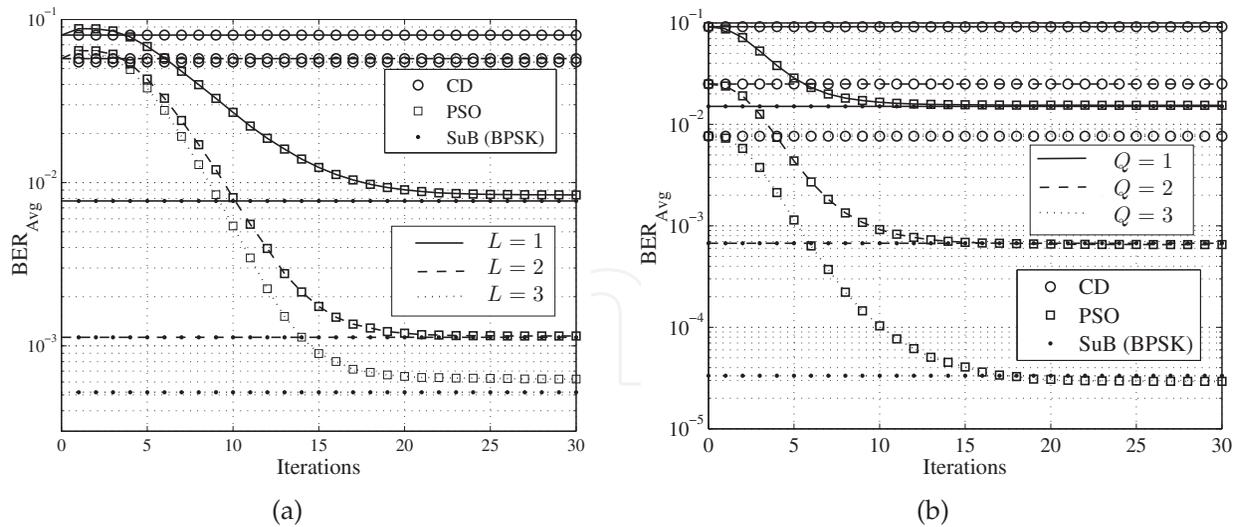(a)   (b)

Fig. 11. Convergence performance of PSO-MUD, with $K = 15$, $E_b/N_0 = 15$, BPSK modulation, (a) under asynchronous multipath slow Rayleigh channels and $I = 3$, for $L = 1$, 2 and 3 paths; and (b) synchronous flat Rayleigh channel, $I = 1$ and $Q = 1$, 2, 3 antennas.

error estimation, which are modeled through the continuous uniform distributions $\mathcal{U}[1 \pm \epsilon]$ centralized on the true values of the coefficients, resulting

$$\widehat{\gamma}_{k,\ell}^{(i)} = \mathcal{U}[1 \pm \epsilon_\gamma] \times \gamma_{k,\ell}^{(i)}; \quad \widehat{\theta}_{k,\ell}^{(i)} = \mathcal{U}[1 \pm \epsilon_\theta] \times \theta_{k,\ell}^{(i)}, \tag{22}$$

where ϵ_γ and ϵ_θ are the maximum module and phase normalized errors for the channel coefficients, respectively. For a low-moderate SNR and medium system loading ($\mathcal{L} = 15/31$), Fig. 12 shows the performance degradation of the PSO-MUD considering BPSK modulation, $L = 1$ and $L = 2$ paths or $Q = 1$ and $Q = 2$ antennas, with estimation errors of order of 10% or 25%, i.e., $\epsilon_\gamma = \epsilon_\theta = 0.10$ or $\epsilon_\gamma = \epsilon_\theta = 0.25$, respectively. Note that PSO-MUD reaches the SuB in both conditions with perfect channel estimation, and the improvement is more evident when the diversity gain increases. However, note that, with spatial diversity, the gain is higher, since the average energy is equally distributed among antennas, while for path diversity is considered a realistic exponential power-delay profile. Moreover, there is a SNR gain of $+3$ dB in the E_b/N_0 for each additional receive antenna. Although there is a general performance degradation when the error in channel coefficient estimation increases, PSO-MUD still achieves much better performance than the CD under any error estimation condition, being more evident for larger number of antennas.

As expected from previous results for flat Rayleigh channel, Fig. 13 shows the performance degradation CD for path ($L = 1$ and $L = 2$) and spatial ($Q = 1$ and $Q = 2$) diversity as function of number of users K. It is evident that the PSO-MUD performance is superior when diversity is exploited. As can be seen, independently of the loading and number of paths, PSO-MUD always accomplishes a much better performance.

In the new generations of wireless systems, beyond spatial and path diversity, the high-order modulation is also explored. Hence, since PSO-MUD must work efficiently for other modulation constellation, Fig. 14 shows the convergence for three different modulations: (a) BPSK, (b) QPSK, and (c) 16-QAM. It is worth mentioning, as presented in Table 2, that the PSO-MUD optimized parameters is specific for each modulation format.
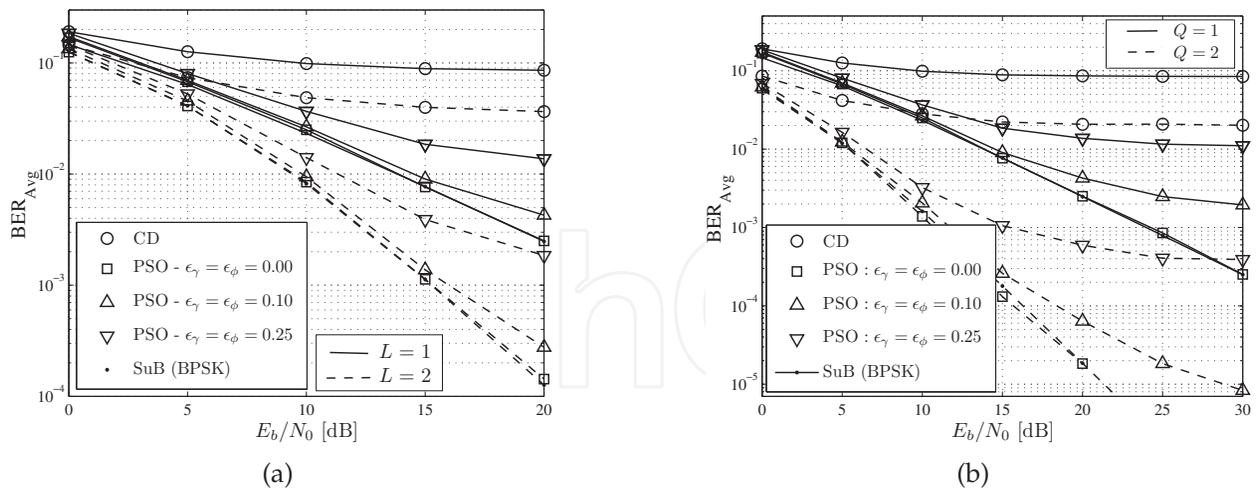
Fig. 12. Performance of PSO-MuD with $K = 15$, BPSK modulation and error in the channel estimation, for a system with (a) path and (b) spatial diversity.
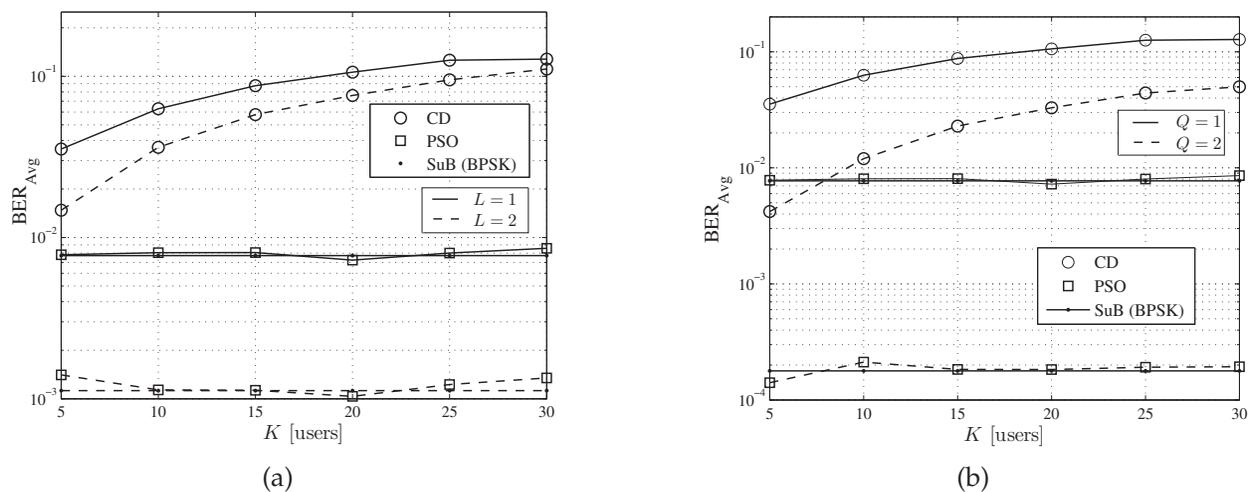

Fig. 13. Performance of PSO-MuD with $E_b/N_0 = 15$ dB and BPSK modulation, for a system with (a) path and (b) spatial diversity.

Similar results are obtained for E_b/N_0 curves in QPSK and 16-QAM cases. Nevertheless, Fig. 15 shows that for 16-QAM modulation with $\phi_1 = 6$, $\phi_2 = 1$, the PSO-MuD performance degradation is quite slight in the range ($0 < \mathcal{L} \leq 0.5$), but the performance is hardly degraded in medium to high loading scenarios.

3. Resource allocation problem

This Section discusses the rate resource allocation with power constraint in multiple access multi-class networks under heuristic optimization perspective. Multirate users associated with different types of traffic are aggregated to distinct user' classes, with the assurance of minimum target rate allocation per user and QoS. Therein, single-objective optimization (SOO) methodology under swarm intelligence approach was carried out aiming to achieve newsworthy performance-complexity tradeoffs. The results are promising in terms of sum
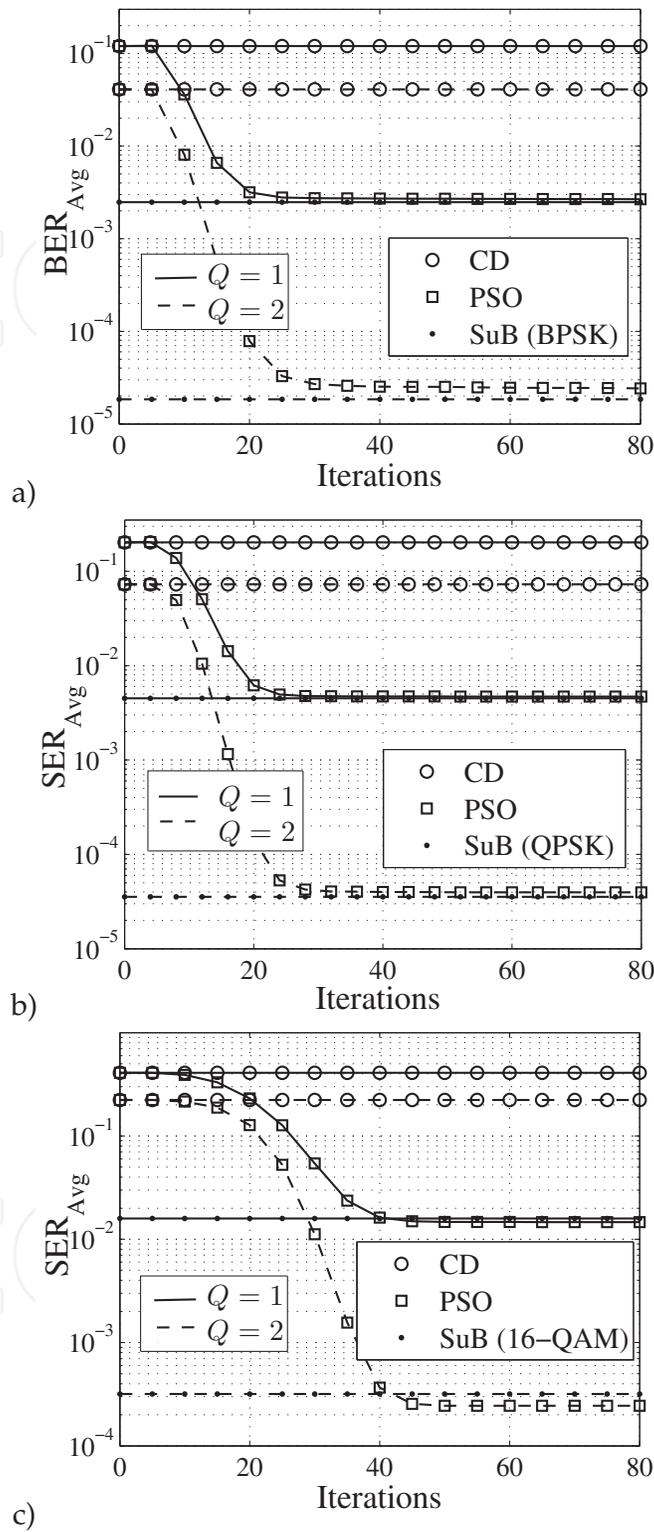
Fig. 14. Convergence of PSO-MUD under flat Rayleigh channel, $E_b/N_0 = 20$ dB, and a) $K = 24$ users with BPSK modulation, b) $K = 12$ users with QPSK modulation and c) $K = 6$ users with 16-QAM modulation
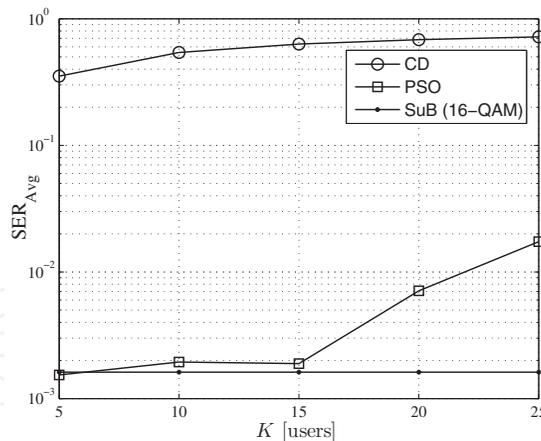
Fig. 15. PSO-MuD and CD performance degradation × system loading under flat Rayleigh channel. 16-QAM modulation and $\phi_1 = 6$, $\phi_2 = 1$.

rate maximization while simultaneously minimizing the total power allocated to each multirate mobile terminal.

3.1 Power-rate allocation problem

In a multiple access system, such as DS/CDMA, the power control problem is of great importance in order to achieve relevant system capacity[5] and throughput. The power allocation issue can be solved by finding the best vector that contains the minimum power to be assigned in the next time slot to each active user, in order to achieve the minimum quality of service (QoS) through the minimum carrier to interference ratio (CIR) allowable.

In multirate multiple access wireless communications networks, the bit error rate (BER) is often used as a QoS measure and, since the BER is directly linked to the signal to interference plus noise ratio (SINR), this parameter can be used as the QoS measurement. Hence, associating the SINR to the CIR at iteration t results:

$$\delta_i[t] = \frac{R_c}{R_i[t]} \times \Gamma_i[t], \qquad t = 0, 1, \ldots \mathcal{G} \tag{23}$$

where $\delta_i[t]$ is the SINR of user i at the tth iteration, R_c is the chip rate and approximately equal to the system's spreading bandwidth; $R_i[t]$ is the data rate for user i, $\Gamma_i[t]$ is the CIR for user i at iteration t, and $\mathcal{G}$ is the maximal number of iterations.

In multirate DS/CDMA systems with multiple processing gains (MPG), where each user class has a different processing gain $\mathsf{G} > 1$, defined as a function of the chip rate by

$$\mathsf{G}_i^\ell = \frac{R_c}{R_i^\ell}, \qquad \ell = 1, 2, \ldots, L, \tag{24}$$

where L is the number of total user's classes defined in the system (voice, data, video). Hence, in MPG-DS/CDMA multiple access systems, the SINR and CIR for the ℓth user's class are related to the processing gain of that service class: $\delta_i^\ell = \mathsf{G}_i^\ell \times \Gamma_i$.

From (23), the data rate for user i at iteration n can be calculated as:

$$R_i[t] = \frac{R_c}{\delta_i[t]} \times \Gamma_i[t], \qquad t = 0, 1, \ldots, \mathcal{G} \tag{25}$$

---

[5] In this chapter the term capacity is employed to express the total number of active users in the system.

The CIR for the ith user can be calculated as Elmusrati & Koivo (2003); Gross et al. (2010):

$$\Gamma_i[t] = \frac{p_i[t]g_{ii}[t]}{\sum\limits_{\substack{j=1 \\ j \neq i}}^{K} p_j[t]g_{ij}[t] + \sigma^2}, \qquad i = 1, \dots, K \tag{26}$$

where $p_i[t]$ is the power allocated to the ith user at iteration t and is bounded by $P_{\max}$, the channel gain (including path loss, fading and shadowing effects) between user j and user (or base station) i is identified by g_{ij}, K is the number of active users in the system (considering all user's classes), and $\sigma_i^2 = \sigma_j^2 = \sigma^2$ is the average power of the additive white Gaussian noise (AWGN) at the input of ith receiver, admitted identical for all users. Therefore, in DS/CDMA multirate systems the CIR relation to achieve the target rate can be calculated to each user class as follows Elmusrati et al. (2008):

$$\Gamma_{\min}^{\ell} = \frac{R_{\min}^{\ell} \delta^*}{R_c}, \qquad \ell = 1, \dots, L \tag{27}$$

where $\Gamma_{\min}^{\ell}$ and $R_{\min}^{\ell}$ is the minimum CIR and minimum user rate[6] associated to the ℓth user class, respectively, δ^* is the minimum (or target) signal to noise ratio (SNR) to achieve minimum acceptable BER (or QoS). Besides, the power allocated to the kth user belonging to the ℓth class at nth iteration is

$$p_k^{\ell}[t], \qquad k = 1, \dots, K_{\ell}; \quad \ell = 1, \dots, L. \tag{28}$$

Hence, the total number of active users in the system is given by $K = K_1 \cup \dots \cup K_{\ell} \cup \dots \cup K_L$. Note that indexes associated to the K users are obtained by concatenation of ascending rates from different user's classes. Thus, K_1 identifies the lowest user's rate class, and K_L the highest.

The $K \times K$ channel gain matrix, considering path loss, shadowing and fading effects, between user j and user i (or base station) is given by

$$\mathbf{G} = \begin{bmatrix} g_{11} & g_{12} & \cdots & g_{1K} \\ g_{21} & g_{22} & \cdots & g_{2K} \\ \vdots & \vdots & \ddots & \vdots \\ g_{K1} & g_{K2} & \cdots & g_{KK} \end{bmatrix}, \tag{29}$$

which could be assumed static or even dynamically changing over the optimization window (T time slots).

Assuming multirate user classes, the classical power control problem can be adapted to achieve the target rates for each user, simply using the Shannon capacity relation between minimum CIR and target rate in each user class, resulting in

$$\Gamma_{k,\min}^{\ell} = 2^{\frac{R_{k,\min}^{\ell}}{R_c}} - 1 = 2^{r_{k,\min}^{\ell}} - 1 \tag{30}$$

---

[6] Or target rate, for single (fixed) rate systems.

where $r_{i,\min}^{\ell}$ is the normalized minimum capacity for the kth user from ℓth user class, expressed by bits/sec/Hz. This equation can be obtained directly from the Shannon capacity equation

$$r_{i,\min}(\mathbf{p}) = \log_2 \left[1 + \Gamma_{i,\min}(\mathbf{p}) \right] \tag{31}$$

Now, considering a $K \times K$ interference matrix $\mathbf{D}$, with

$$D_{ij} = \begin{cases} 0, & i = j; \\ \dfrac{\Gamma_{i,\min} g_{ji}}{g_{ii}}, & i \neq j; \end{cases} \tag{32}$$

where $\Gamma_{i,\min}$ can be obtained from (27), taking into account each rate class requirement and the column vector $\mathbf{u} = [u_1, u_2, \ldots, u_K]^T$, with elements

$$u_i = \frac{\Gamma_{i,\min} \sigma_i^2}{g_{ii}}, \tag{33}$$

the analytical optimal power vector allocation $\mathbf{p}^* = [p_1, p_2, \ldots, p_K]^T$ can be obtained simply by matrix inversion as:

$$\mathbf{p}^* = (\mathbf{I} - \mathbf{D})^{-1} \mathbf{u} \tag{34}$$

if and only if the maximum eigenvalue of $\mathbf{D}$ is smaller than 1 Seneta (1981); $\mathbf{I}$ is the $K \times K$ identity matrix. In this situation, the power control problem shows a feasible solution.

3.1.1 Fixed-rate power allocation criterion

The classical power allocation problem is extended to incorporate multi but fixed rate criterion in order to guarantee the target data rate per user class[7] while minimizing the total power consumption of mobile terminals. Mathematically, the optimization problem is expressed by:

$$\begin{aligned} \min \quad & \mathbf{p} = \left[p_1^1 \ldots p_{K_1}^1, \ldots, p_1^{\ell} \ldots p_{K_{\ell}}^{\ell}, \ldots, p_1^L \ldots p_{K_L}^L \right] \\ \text{s.t.} \quad & 0 < p_k^{\ell} \leq P_{\max} \\ & R^{\ell} = R_{\min}^{\ell}, \qquad \forall k \in K_{\ell}, \text{ and } \forall \ell = 1, 2, \ldots, L \end{aligned} \tag{35}$$

Under multirate environment, and in order to achieve the QoS to each user class, the recursive resource allocation update must be adapted to reach an equilibrium. Particularly, for power updating process, $\lim_{n \to \infty} p_i[n] = p_i^*$ when the power allocated to each user satisfies the target rate constraint given in (35). Hence, the recursive equation must be rewritten considering SINR per user class, via (23), in order to incorporate multirate scenario. The minimum CIR per user class is obtained directly by (27). In this way, considering the relation between CIR and SINR in a multirate DS/CDMA context, the following equation is employed in order to iteratively solve optimization problem of (35):

$$\begin{aligned} \delta_i[n] &= \mathsf{G}_i^{\ell} \times \Gamma_i[n] \\ &= \mathsf{G}_i^{\ell} \times \frac{p_i[n] g_{ii}[n]}{\sum\limits_{\substack{j=1 \\ j \neq i}}^{K} p_j[n] g_{ij}[n] + \sigma^2}, i = 1, \ldots, K \end{aligned} \tag{36}$$

---

[7] As a consequence, assure the QoS for each user.

where G_i is the spreading factor for the ith user:

$$\mathsf{G}_i = \frac{R_c}{R_i^\ell} \tag{37}$$

For all users from the same user class transmitting at the minimum (of fixed) rate per class, the spreading factor is given by:

$$\mathsf{G}_i = \frac{R_c}{R_{i,\min}^\ell} \tag{38}$$

Note that the CIR of ith user at the nth iteration is weighted by spreading factor; so the corresponding SINR is inversely proportional to the actual (minimum) rate of the ith user of the ℓth class.

Therefore, the single-objective optimization problem in (35) can be slightly modified as:

$$J_1(\mathbf{p}) = \min \sum_{k=1}^{K} p_k \tag{39}$$
$$\text{s.t.} \quad \delta_k \geq \delta_k^*, \qquad 0 < p_k^\ell \leq P_{\max}, \quad \text{and} \quad R^\ell = R_{\min}^\ell$$
$$\forall k \in K_\ell, \text{ and } \forall \ell = 1, 2, \ldots, L$$

or alternatively, the min-max version of (39) could be obtained:

$$J_1(\mathbf{p}) = \min \max_{k=1,\ldots,K} p_k \tag{40}$$
$$\text{s.t.} \quad \delta_k \geq \delta_k^*, \qquad 0 < p_k^\ell \leq P_{\max}, \quad \text{and} \quad R^\ell = R_{\min}^\ell$$
$$\forall k \in K_\ell, \text{ and } \forall \ell = 1, 2, \ldots, L$$

Based on the work of Moustafa et al. (2000), and further results of Elkamchouchi et al. (2007), the above single-objective function could be modified in order to incorporate the near-far aspect; hence the following maximization cost function could be employed as an alternative:

$$J_1(\mathbf{p}) = \max \frac{1}{K} \sum_{k=1}^{K} \mathcal{F}_k^{\text{th}} \left(1 - \frac{p_k}{P_{\max}}\right) + \frac{\rho}{\sigma_{\text{rp}}} \tag{41}$$
$$\text{s.t.} \quad \delta_k \geq \delta_k^*, \qquad 0 < p_k^\ell \leq P_{\max}, \quad \text{and} \quad R^\ell = R_{\min}^\ell$$
$$\forall k \in K_\ell, \text{ and } \forall \ell = 1, 2, \ldots, L$$

where the term $\frac{\rho}{\sigma_{rp}^2}$ gives credit to the solutions with small standard deviation of the normalized (by the inverse of rate factor, G^ℓ) received power distribution:

$$\sigma_{\text{rp}}^2 = \text{var}\left(\mathsf{G}^1 p_1 g_{11}, \mathsf{G}^1 p_2 g_{22}, \ldots, \mathsf{G}^\ell p_k g_{kk}, \ldots, \mathsf{G}^L p_k g_{KK}\right), \tag{42}$$

i.e. the more close the normalized received power values are with other (i.e., small variance of normalized received power vector), the bigger this term. For single-rate DS/CDMA systems, $\mathsf{G}^1 = \ldots = \mathsf{G}^\ell = \ldots = \mathsf{G}^L$.

It is worth to note that since the variance of the normalized received power vector, σ_{rp}^2, normally assumes very small values, the coefficient ρ just also take very small values in order

to the ratio $\rho/\sigma_{\mathrm{rp}}$ achieves a similar order of magnitude of the first term in (41), and will be determined as a function of the number of users, K, and cell geometry (basically, the cell radius). Hence, the term $\rho/\sigma_{\mathrm{rp}}$ has an effective influence in minimizing the near-far effect on CDMA systems, and at the same time it has a non-zero value for all swarm particles Elkamchouchi et al. (2007). Besides, the threshold function in (41) is defined as:

$$\mathcal{F}_k^{th} = \begin{cases} 1, & \delta_k \geq \delta^* \\ 0, & \text{otherwise} \end{cases}$$

with the SINR for the kth user, δ_k, given by (36), and the term $1 - \frac{p_k}{P_{\max}}$ gives credit to solutions that use minimum power and punishes others using high levels Moustafa et al. (2000; 2001a;b).

3.1.2 Throughput maximization for multirate systems under power constraint

The aiming herein is to incorporate multirate criterion with throughput maximization for users with different QoS, while the power consumption constraint at mobile terminals is bounded by a specific value at each user. As a result, the optimization problem can be formulated as a special case of generalized linear fractional programming (GLFP) Phuong & Tuy (2003). So, the following optimization problem can be posed

$$\max \prod_{i=1}^{K} \left[\frac{f_i(\mathbf{p})}{g_i(\mathbf{p})} \right]^{w_i} \tag{43}$$

$$\text{s.t. } 0 < p_i^\ell \leq P_{\max};$$

$$\frac{f_i(\mathbf{p})}{g_i(\mathbf{p})} \geq 2^{r_{i,\min}^\ell}, \qquad \forall i \in K_\ell, \text{ and } \forall \ell = 1, 2, \cdots L$$

where $r_{i,\min}^\ell \geq 0$ is the minimum normalized (by CDMA system bandwidth, R_c) data rate requirement of ith link, including the zero-rate constraint case; and $w_i > 0$ is the priory weight for the ith user to transmit with minimum data rate and QoS guarantees, assumed normalized, so that $\sum_{i=1}^{K} w_i = 1$. Moreover, note that the second constraint in (43) is obtained directly from (30), (26), and (23), where the minimum data rate constraints was transformed into minimum SINR constraints through Shannon capacity equation

$$R_i = R_c \log_2 \left[1 + \theta^{\mathrm{BER}_i} \mathrm{G}_i^\ell \times p_i g_{ii} \times \left(\sum_{j \neq i}^{K} p_j g_{ij} + \sigma^2 \right)^{-1} \right], \tag{44}$$

for $i = 1, \ldots, K$, with $\theta^{\mathrm{BER}_i} = -\frac{1.5}{\log(5\,\mathrm{BER}_i)}$, BER_i is the maximal allowed bit error rate for user i,

$$f_i(\mathbf{p}) = \theta^{\mathrm{BER}_i} \mathrm{G}_i^\ell \times p_i g_{ii} + \sum_{\substack{j=1 \\ j \neq i}}^{K} p_j g_{ij} + \sigma^2, \text{ and } \quad g_i(\mathbf{p}) = \sum_{\substack{j=1 \\ j \neq i}}^{K} p_j g_{ij} + \sigma^2 \tag{45}$$

for $i = 1, \ldots, K$. The objective function in (43) is a product of exponentiated linear fractional functions, and the function $\prod_{i=1}^{K}(z_i)^{w_i}$ is an increasing function on K-dimensional nonnegative

real domain Li Ping Qian (2009). Furthermore, the optimization problem (43) can be rewritten using the basic property of the logarithmic function, resulting in

$$
\begin{aligned}
J(\mathbf{p}) = \max_{\mathbf{p}} \sum_{i=1}^{K} w_i \left[\log_2 f_i(\mathbf{p}) - \log_2 g_i(\mathbf{p}) \right] \;=\; \max \sum_{i=1}^{K} w_i \left[\widetilde{f}_i(\mathbf{p}) - \widetilde{g}_i(\mathbf{p}) \right] \\
\text{s.t.} \quad 0 < p_i^\ell \leq P_{\max}; \\
\widetilde{f}_i(\mathbf{p}) - \widetilde{g}_i(\mathbf{p}) \geq r_{i,\min}^\ell, \qquad \forall i \in K_\ell, \; \ell = 1, 2, \cdots L
\end{aligned}
\tag{46}
$$

3.1.3 Quality of solution × convergence speed

The quality of solution achieved by any iterative resource allocation procedure could be measured by how close to the optimum solution is the found solution, and can be quantified by means of the normalized mean squared error (NMSE) when equilibrium is reached. For power allocation problem, the NMSE definition is given by

$$
NSE[t] = \mathbb{E}\left[\frac{\|\mathbf{p}[t] - \mathbf{p}^*\|^2}{\|\mathbf{p}^*\|^2} \right],
\tag{47}
$$

where $\| \cdot \|^2$ denotes the squared Euclidean distance to the origin, and $\mathbb{E}[\cdot]$ the expectation operator.

3.2 Continuous PSO algorithm for resource allocation wireless networks

In this section, a different approach for throughput maximization under power constraint problems, described by (46) will be considered using swarm intelligence optimization method Kennedy & Eberhart (2001). Single-objective optimization (SOO) approach was adopted. The convexation of the original multi-class throughput maximization problem, obtained in (46), is employed hereafter as cost function for the PSO.

The problem described in (46) indicated an optimization developed in the $\mathbb{R}$ set. Hence, in the PSO strategy, each candidate power-vector defined as $\mathbf{b}_p[t]$, of size[8] K, is used for the velocity calculation of next iteration

$$
\mathbf{v}_p[t+1] = \omega[t] \cdot \mathbf{v}_p[t] + \phi_1 \cdot \mathbf{U}_{p_1}[t](\mathbf{b}_p^{\text{best}}[t] - \mathbf{b}_p[t]) + \phi_2 \cdot \mathbf{U}_{p_2}[t](\mathbf{b}_g^{\text{best}}[t] - \mathbf{b}_p[t])
\tag{48}
$$

where $\omega[t]$ is the inertia weight of the previous velocity in the present speed calculation; $\mathbf{U}_{p_1}[t]$ and $\mathbf{U}_{p_2}[t]$ are diagonal matrices with dimension K, and elements are random variables with uniform distribution $\sim \mathcal{U} \in [0,1]$, generated for the pth particle at iteration $t = 1, 2, \ldots, \mathcal{G}$; $\mathbf{b}_g^{\text{best}}[t]$ and $\mathbf{b}_p^{\text{best}}[t]$ are the best global position and the best local positions found until the tth iteration, respectively; ϕ_1 and ϕ_2 are acceleration coefficients regarding the best particles and the best global positions influences in the velocity update, respectively.

The particle(s) selection for evolving under power-multirate adaptation strategy is based on the lowest fitness values satisfying the constraints in (46). The pth particle's position at iteration t is a power candidate-vector $\mathbf{b}_p[t]$ of size $K \times 1$. The position of each particle is updated using the new velocity vector (48) for that particle

$$
\mathbf{b}_p[t+1] = \mathbf{b}_p[t] + \mathbf{v}_p[t+1], \qquad i = 1, \ldots, \mathcal{P}
\tag{49}
$$

---

[8] Remember, as defined previously, for multirate power optimization problem: $K = K_1 \cup \ldots \cup K_\ell \cup \ldots \cup K_L$.

The PSO algorithm consists of repeated application of the update velocity and position update equations. A pseudo-code for the single-objective continuous PSO power-multirate allocation problem is presented in Algorithm 2.

Algorithm 2 SOO Continuous PSO Algorithm for the Power-Multirate Allocation Problem

---

Input: $\mathcal{P}, \mathcal{G}, \omega, \phi_1, \phi_2, V_{\max}$;   **Output:** $\mathbf{p}^*$

begin
1. initialize first population: $t = 0$;
        $\mathbf{B}[0] \sim \mathcal{U}[P_{\min}; P_{\max}]$
        $\mathbf{b}_p^{\text{best}}[0] = \mathbf{b}_p[0]$ and $\mathbf{b}_g^{\text{best}}[0] = \mathbf{P}_{\max}$;
        $\mathbf{v}_p[0] = \mathbf{0}$: null initial velocity;
2. while $n \leq N$
        a. calculate $J(\mathbf{b}_p[t])$, $\forall \mathbf{b}_p[t] \in \mathbf{B}[t]$ using (46);
        b. update velocity $\mathbf{v}_p[t]$, $p = 1, \ldots, \mathcal{P}$, through (48);
        c. update best positions:
            for $p = 1, \ldots, \mathcal{P}$
              if $J(\mathbf{b}_p[t]) < J(\mathbf{b}_p^{\text{best}}[t]) \wedge R_p[t] \geq r_{p,\min}$,
                   $\mathbf{b}_p^{\text{best}}[t+1] \leftarrow \mathbf{b}_p[t]$
              else $\mathbf{b}_p^{\text{best}}[t+1] \leftarrow \mathbf{b}_p^{\text{best}}[t]$
            end
            if $\exists\, \mathbf{b}_p[t]$ such that $\left[J(\mathbf{b}_p[t]) < J(\mathbf{b}_g^{\text{best}}[t])\right] \wedge R_p[t] \geq r_{p,\min}$
                        $\wedge \left[J(\mathbf{b}_p[t]) \leq J(\mathbf{b}_p'[n]), \ \forall\, p' \neq p\right]$,
            $\mathbf{b}_g^{\text{best}}[t+1] \leftarrow \mathbf{b}_p[t]$
            else $\mathbf{b}_g^{\text{best}}[t+1] \leftarrow \mathbf{b}_g^{\text{best}}[t]$
        d. Evolve to a new swarm population $\mathbf{B}[t+1]$, using (46);
        e. set $t = t + 1$.
        end
3. $\mathbf{p}^* = \mathbf{b}_g^{\text{best}}[\mathcal{G}]$.
end

— —

$\mathcal{P}$: population size.
$\mathbf{B} = [\mathbf{b}_1, \ldots, \mathbf{b}_p, \ldots, \mathbf{b}_{\mathcal{P}}]$ particle population matrix, dimension $K \times \mathcal{P}$.
$\mathcal{G}$: maximum number of swarm iterations.
$\mathbf{P}_{\max}$: maximum power vector considering each mobile terminal rate class.

In order to reduce the likelihood that the particle might leave the search universe, maximum velocity $V_{\max}$ factor is added to the PSO model (48), which will be responsible for limiting the velocity in the range $[\pm V_{\max}]$. The adjustment of velocity allows the particle to move in a continuous but constrained subspace, been simply accomplished by

$$v_p[t] = \min\left\{V_{\max}; \max\left\{-V_{\max}; v_p[t]\right\}\right\} \tag{50}$$

From (50) it's clear that if $|v_p[t]|$ exceeds a positive constant value $V_{\max}$ specified by the user, the pth particle' velocity is assigned to be $\text{sign}(v_p[t])V_{\max}$, i.e. particles velocity on each of $K-$dimension is clamped to a maximum magnitude $V_{\max}$. If the search space could be defined by the bounds $[P_{\min}; P_{\max}]$, then the value of $V_{\max}$ will be typically set so that $V_{\max} = \tau(P_{\max} - P_{\min})$, where $0.1 \leq \tau \leq 1.0$, please refer to Chapter 1 within the definition of reference Nedjah & Mourelle (2006).

To elaborate further about the inertia weight it can be noted that a relatively larger value of w is helpful for global optimum, and lesser influenced by the best global and local positions[9], while a relatively smaller value for w is helpful for convergence, i.e., smaller inertial weight encourages the local exploration as the particles are more attracted towards $\mathbf{b}_p^{\text{best}}$ and $\mathbf{b}_g^{\text{best}}$ Eberhart & Shi (2001); Shi & Eberhart (1998).

Hence, in order to achieve a balance between global and local search abilities, a linear inertia weight decreasing with the algorithm evolving, having good global search capability at beginning and good local search capability latter, was adopted herein

$$w[n] = (w_{\text{initial}} - w_{\text{final}}) \cdot \left(\frac{N - n}{N} \right)^m + w_{\text{final}} \tag{51}$$

where w_{initial} and w_{final} is the initial and final weight inertia, respectively, $w_{\text{initial}} > w_{\text{final}}$, N is the maximum number of iterations, and $m \in [0.6; 1.4]$ is the nonlinear modulation index Chatterjee & Siarry (2006).

3.2.1 PSO Parameters optimization for resource allocation problem

For power-rate resource allocation problem, simulation experiments were carried out in order to determine the suitable values for the PSO input parameters, such as acceleration coefficients, ϕ_1 and ϕ_2, maximal velocity factor, V_{max}, weight inertia, ω, and population size, $\mathcal{P}$, regarding the throughput multirate optimization problem.

Under discrete optimization problems, such as DS/CDMA multiuser detection, it is known that fast PSO convergence without losing certain exploration and exploitation capabilities could be obtained increasing the parameter ϕ_2 Oliveira et al. (2006) while holding ϕ_1 into the low range values. However, for the continuous optimization problem investigated herein, numerical results presented in Section 3.3.1 indicate that after an enough number of iterations ($\mathcal{G}$) for convergence, the maximization of cost function were obtained within low values for both acceleration coefficients.

The V_{max} factor is then optimized. The diversity increases as the particle velocity crosses the limits established by $[\pm V_{\text{max}}]$. The range of V_{max} determines the maximum change one particle can take during iteration. Without inertial weight ($w = 1$), Eberhart and Shi Eberhart & Shi (2001) found that the maximum allowed velocity V_{max} is best set around 10 to 20% of the dynamic range of each particle dimension. The appropriate choose of V_{max} avoids particles flying out of meaningful solution space. Herein, for multirate DS/CDMA rate allocation problem, a non exhaustive search has indicated that the better performance$\times$complexity trade-off was obtained setting the maximal velocity factor value to $V_{\text{max}} = 0.2 \times (P_{\text{max}} - P_{\text{min}})$.

For the inertial weight, ω, simulation results has confirmed that high values imply in fast convergence, but this means a lack of search diversity, and the algorithm can easily be trapped in some local optimum, whereas a small value for ω results in a slow convergence due to excessive changes around a very small search space. In this work, it was adopted a variable ω, as described in (51), but with $m = 1$, and initial and final weight inertia setting up to $w_{\text{initial}} = 1$ and $w_{\text{final}} = 0.01$. Hence, the initial and final maximal velocity excursion values

---

[9] Analogous to the idea of the phenomenon that it is difficult to diverge heavier objects in their flight trajectory than the lighter ones.

were bounded through the initial and final linear inertia weight multiplied by V_m, adopted as a percentage of the maximal and minimal power difference values

$$w_\mathrm{initial} \times V_\mathrm{max} = 0.2 \left(P_\mathrm{max} - P_\mathrm{min}\right), \qquad \text{and} \qquad w_\mathrm{final} \times V_\mathrm{max} = 0.002 \left(P_\mathrm{max} - P_\mathrm{min}\right) \quad (52)$$

Finally, stopping criterion can be the maximum number of iterations (velocity changes allowed for each particle) or reaching the minimum error threshold, e.g.,

$$\left| \frac{J[t] - J[t-1]}{J[t]} \right| < \epsilon_\mathrm{stop} \tag{53}$$

where typically $\epsilon_\mathrm{stop} \in [0.001; 0.01]$.

Alternately, the convergence test can be evaluated through the computation of the average percent of success[10], taken over T runs to achieve the global optimum, and considering a fixed number of iterations N. A test is considered 100% successful if the following relation holds:

$$|J[\mathcal{G}] - J[\mathbf{p}^*]| < \epsilon_1 J[\mathbf{p}^*] + \epsilon_2 \tag{54}$$

where, $J[\mathbf{p}^*]$ is the global optimum of the objective function under consideration, $J[\mathcal{G}]$ is the optimum of the objective function obtained by the algorithm after N iterations, and ϵ_1, ϵ_2 are accuracy coefficients, usually in the range $[10^{-6}; 10^{-2}]$. In this study it was assumed that $TR = 100$ trials and $\epsilon_1 = \epsilon_2 = 10^{-2}$.

3.3 Numerical results

In order to validate the proposed swarm optimization approach in solving resource allocation problems on multiple access CDMA wireless networks, simulations were carried out with system parameters indicated in Table 5. In all simulation results discussed in this section, it was assumed a retangular multicell geometry with a number of base station (BS) equal to 4 and mobile terminals (mt) uniformly distributed over $25Km^2$ area. Besides, the initial rate assignment for all multirate users was admitted discretely and uniformly distributed over three chip rate submultiple, $R_\mathrm{min} = [\frac{1}{128}; \frac{1}{32}; \frac{1}{16}]R_c$ [bps].

A number of mobile terminals ranging from $K = 5$ to 250 was considered, which experiment slow fading channels, i.e., the following relation is always satisfied

$$T_\mathrm{slot} < (\Delta t)_c \tag{55}$$

where $T_\mathrm{slot} = R_\mathrm{slot}^{-1}$ is the time slot duration, R_slot is the transmitted power vector update rate, and $(\Delta t)_c$ is the coherence time of the channel[11]. This condition is part of the SINR estimation process, and it implies that each power updating accomplished by the DPCA happens with rate of R_slot, assumed here equal to 1500 updates per second.

The optimization process $J(\mathbf{p})$ in (46) should converge to the optimum point before each channel gain g_{ij} experiments significant changing. Note that satisfying (55) the gain matrices remain approximately static during one convergence process interval, i.e., 666.7μs.

In all of the simulations the entries values for the QoS targets were fixed in $\delta^* = 4$ dB, the adopted receiver noise power for all users is $P_n = -63$ dBm, and the gain matrix $\mathbf{G}$ have intermediate values between those used in Uykan & Koivo (2004.) and Elmusrati et al. (2008).

---

[10] In terms of the PSO algorithm achieves full convergence.

[11] Corresponds to the time interval in which the channel characteristics do not suffer expressive variations.

Parameters	Adopted Values
DS/CDMA Power-Rate Allocation System	
Noise Power	$P_n = -63$ [dBm]
Chip rate	$R_c = 3.84 \times 10^6$
Min. Signal-noise ratio	$SNR_{\min} = 4$ dB
Max. power per user	$P_{\max} \in [30, 35]$ [dBm]
Min. Power per user	$P_{\min} = SNR_{\min} + P_n$ [dBm]
Time slot duration	$T_{\text{slot}} = 666.7\mu s$ or $R_{\text{slot}} = 1500$ slots/s
# mobile terminals	$K \in [5, 250]$
# base station	BS $= 4$
Cell geometry	rectangular, with $x_{\text{cell}} = y_{\text{cell}} = 5$ Km
Mobile term. distrib.	$\sim \mathcal{U}[x_{\text{cell}}, y_{\text{cell}}]$
Fading Channel Type	
Path loss	$\propto d^{-2}$
Shadowing	uncorrelated log-normal, $\sigma^2 = 6$ dB
Fading	Rice: [0.6; 0.4]
Max. Doppler freq.	$f_{D\max} = 11.1$ Hz
Time selectivity	slow
User Types	
# user classes	$L = 3$ (voice, video, data)
User classes Rates	$R_{\min} = [\frac{1}{128}; \frac{1}{32}; \frac{1}{16}]R_c$ [bps]
User classes BER	$\theta^{\text{BER}} = [5 \times 10^{-3}; 5 \times 10^{-5}; 5 \times 10^{-8}]$
Swarm Power-Rate Algorithm	
Accel. Coefs.	$\phi_1 = 1\ \phi_2 = 2$
Max. veloc. factor	$V_m = 0.2 \times (P_{\max} - P_{\min})$
Weight inertia (linear decay)	$w_{\text{initial}} = 1; w_{\text{final}} = 0.01$
Population Size	$\mathcal{P} = K + 2$
Max. # iterations	$\mathcal{G} \in [500, 2000]$
Simulation Parameter	
Trials number	$TR = 1000$ samples

Table 5. Multirate DS/CDMA system parameters

Finally, the PSO resource allocation performance analysis was characterized considering static channels condition. In this scenario, the channel coefficients remain constant during all the convergence process (N iterations), i.e., for a time interval equal or bigger than T_{slot}. However, the extension of the presented numerical results to dynamic channels is straightforward.

3.3.1 Numerical results for the multirate SOO throughput maximization

A parameters analysis was done in order to determine the best combination of ϕ_1 and ϕ_2 parameters under multirate SOO throughput maximization problem. Simulations were carried out using the same configuration, i.e., channel conditions, number of users in the system, users QoS requirements and users services classes.

Table 6 and Fig. 16 illustrate the different solution qualities in terms of cost function value, when different values for ϕ_1 and ϕ_2 are combined in a system with $K = 5$ users. The average cost function values where taken as the average over 1000 trials. Furthermore, the cost function values showed in Table 6 were obtained at the 1000th iteration. User's rates were assigned following just one class rate: $R_{\min} = \frac{1}{128}R_c$ [bps].

From Table 6 and Fig. 16 it is clear that for $K = 5$ users the parameters $\phi_1 = 2$ and $\phi_2 = 1$ result in an average cost function value higher than other configurations at the 1000th iteration. Thus, the use of this parameters for a small system loading is the best in terms of rate-power

(ϕ_1, ϕ_2)	$(1,2)$	$(2,1)$	$(2,2)$	$(4,2)$	$(2,8)$	$(8,2)$
$J[\mathcal{G}]$	4.2866	4.3131	4.2833	4.3063	4.2532	4.3091

$\mathcal{G} = 1000$ Its, average value taken over 1000 trials.

Table 6. Acceleration coefficients choice for $K = 5$ users, single-rate problem.

allocation optimization problem. It is worth to note that the differences between the results shown in Table 6 are equivalent to a sum rate difference raging from $\Delta\Sigma_R = 60$ kbps to $\Delta\Sigma_R = 670$ kbps, Fig. 16.
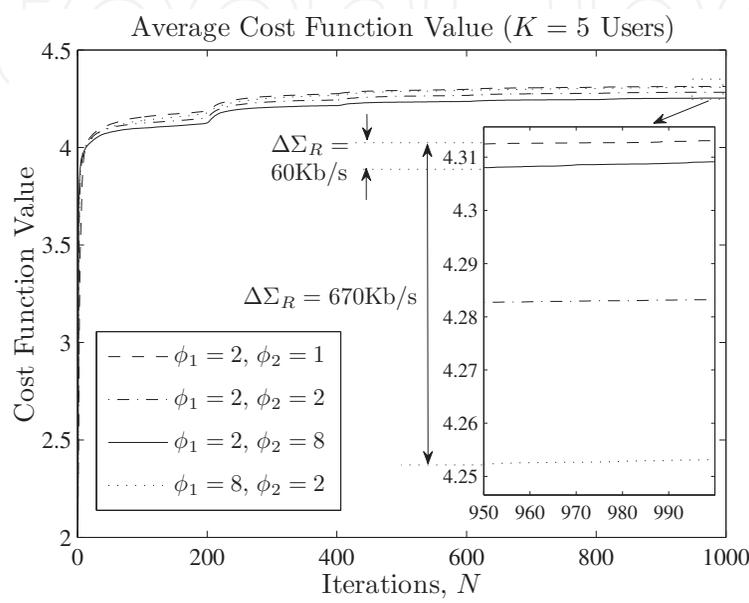
Fig. 16. Cost function evolution through 1000 iterations, averaged over 1000 realizations. $K = 5$ users under the same channel conditions for different ϕ_1 and ϕ_2 parameters.

Figures 17.a) and 17.b) show typical sum rate and sum power allocation evolution through iterations with $K = 20$ users, $\phi_1 = 2$ and $\phi_2 = 1$ and population size $M = K + 2$. Observe that the power allocation updates after ≈ 385th iteration are almost insignificant in terms of sum rate values. This happens due to the small increments on each user rate, ranging from 1 to 10 Kbps, when compared to the system throughput.

The proposed algorithm has been found robust under a high number of multirate active users in the system. Figures 18.a) and 18.b) show typical sum rate and sum power allocation evolution through iterations for $K = 100$ users. As expected, the algorithm needs more iterations to achieve convergence (around 500 iterations), regarding to $K = 20$ users case, but the gain in terms of throughput increasing combined to power reduction after optimization is significant.

Additionally, a small increase in the maximum power per user, i.e. from 30dBm to 35dBm, allows the algorithm to easily find a solution to the throughput optimization problem for a huge system loading, i.e 250 multirate users in a $25Km^2$ rectangular cell geometry. Figures 19.a) and 19.b show a typical sum power and sum rate evolution through iterations for $K = 250$ users. Observe that the algorithm achieves convergence around 750 iterations, which implies that convergence speed, in terms of iterations, grows with the number of active users in the system.
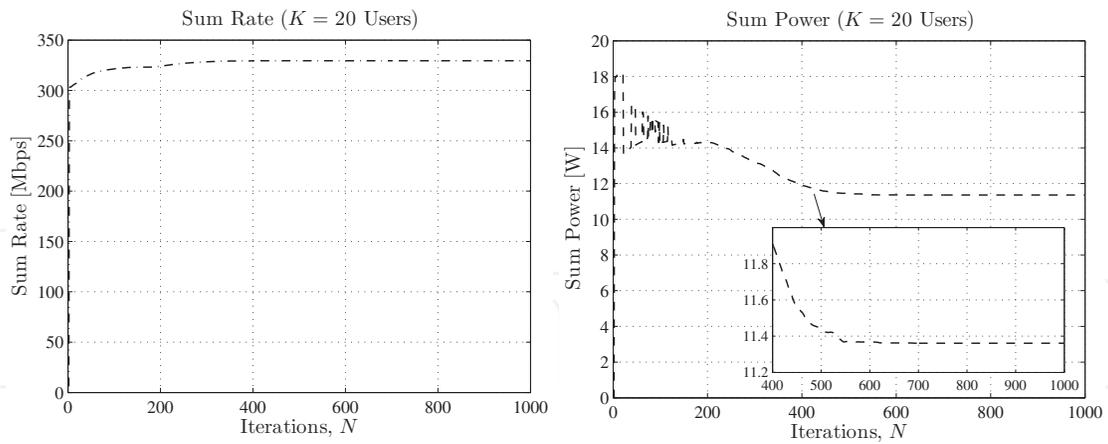
Fig. 17. Typical a) sum rate and b) sum power evolution with $\phi_1 = 1, \phi_2 = 2$, and $K = 20$ users.
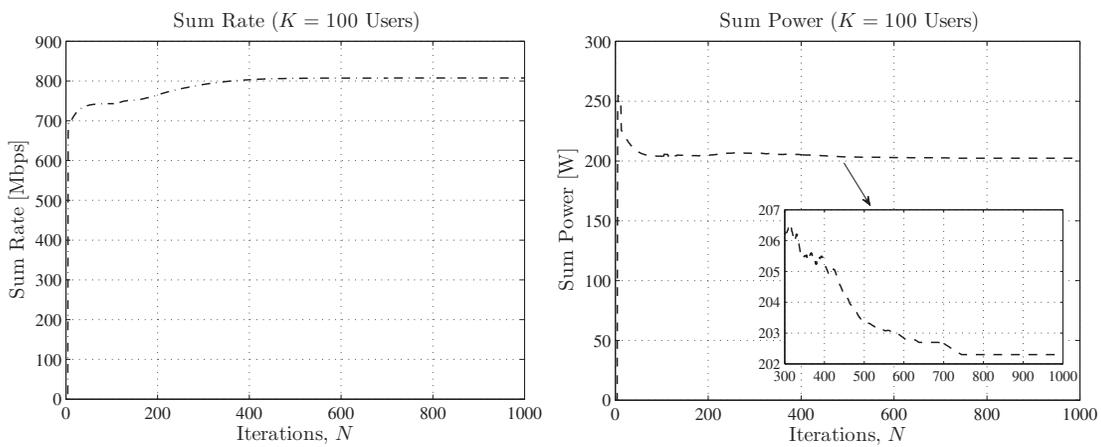

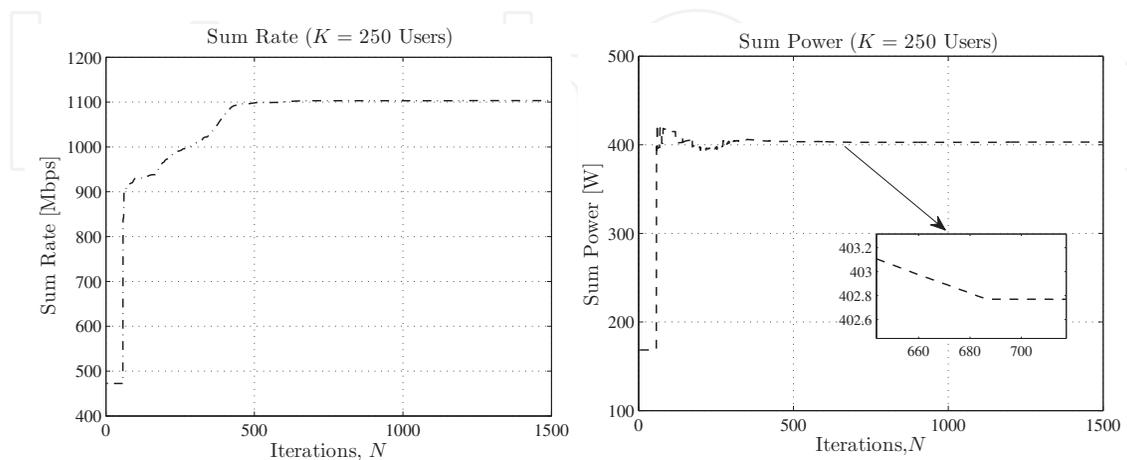Fig. 18. Typical a) sum rate and b) sum power evolution with $\phi_1 = 1, \phi_2 = 2$, and $K = 100$ users.

Fig. 19. Typical a) sum rate and b) sum power evolution with, $\phi_1 = 1, \phi_2 = 2$, $P_{\max} = 35\text{dBm}$ per user, and $K = 250$ users.

3.3.2 Numerical results for the multirate fixed-rate power minimization

In the following subsections there will be discussed aspects of parameters optimization for the obtained simulation results, also presented herein.

3.3.2.1 Convergence aspects: ϕ_1 and ϕ_2 optimization

Simulation experiments were carried out in order to determine a good choice for acceleration coefficients ϕ_1 and ϕ_2 regarding the power multirate optimization problem. Table 7 illustrates different solution qualities in terms of the NMSE, when different values for ϕ_1 and ϕ_2 are combining in a system with different number of users K. Systems with single-rate and multi-rate as well were considered. The NMSE values where taken as the average over 100 trials. Besides, the NMSE convergence values were taken after $N = 800$ iterations for single-rate (SR) systems with $K = 25$ users, and $N = 1000$ iterations for multi-rate (MR) systems with $K = 10$ users. User's rates were randomly assigned following three classes rate: $R_{\min} = [\frac{1}{128}; \frac{1}{32}; \frac{1}{16}]R_c$ [bps].

Note that for multi-rate scenarios the optimal acceleration coefficient values change. Hence, considering the solution quality, it was found $\phi_1 = 1.2$ and $\phi_2 = 0.6$ for single-rate power optimization problem, and $\phi_1 = 2$ and $\phi_2 = 2$ for multi-rate systems high dimensional ($K \geq 10$) power optimization. For $K < 10$ the best convergence $\times$ solution quality trade-off was achieved with $\phi_1 = 1$ and $\phi_2 = 2$.

(ϕ_1, ϕ_2)	$(1.2, 0.6)$	$(2, 2)$	$(6, 2)$	$(8, 2)$	$(1, 2)$	$(0.8, 2)$
$NMSE_{\text{SR}}$	$10^{-1.5}$	$10^{-1.2}$	$10^{0.75}$	$10^{2.25}$	10^{-1}	$10^{-0.9}$
$NMSE_{\text{MR}}$	$10^{0.9}$	$10^{-1.3}$	10^{2}	$10^{2.1}$	$10^{-0.8}$	10^{-1}

SR: $N = 800$ Its; $K = 25$ users; MR: $N = 1000$ Its; $K = 10$ users

Table 7. Coarse optimization results for ϕ_1 and ϕ_2 parameters considering single-rate (SR) and multi-rate (MR) systems.

Results have shown that the algorithm achieves convergence to the optimal (analytical) solution for a wide range of number of users, cell geometries and channel conditions. Figure 20 shows the P_g^{best} vector evolution through the 800 iterations for two different acceleration coefficient configurations under $K = 5$ users. The algorithm reaches convergence around 550-600 iterations for the left graphs and 350-375 iterations under $\phi_1 = 1.0$, $\phi_2 = 2.0$ (right). Simulations revealed that increasing ϕ_2 or reducing $\phi_1 < 1.0$ causes the non-convergence of the algorithms. Additionally, parameters $\phi_1 = 1.0$ and $\phi_2 = 2.0$ result in an $\approx 45\%$ faster convergence when compared to parameters $\phi_1 = 2.0$, $\phi_2 = 2.0$. In the other hand the NMSE and the normalized square error (NSE)[12] for faster convergence is higher than for the slower convergence parameters.

Additionally, for low-medium system loading ($K < 10$ users) further simulations revealed that parameters $\phi_1 = 1.0$ and $\phi_2 = 2.0$ result in an $\approx 45\%$ faster convergence when compared to parameters $\phi_1 = 2.0$, $\phi_2 = 2.0$. However, when $K > 13$, Figure 21 shows that the best values for the local and global acceleration factors are $\phi_1 = 1$ and $\phi_2 = 2$, while for $K \leq 13$ the best combination confirms the values $\phi_1 = 2$ and $\phi_2 = 2$. Besides, the NSE for $K > 20$ users is almost constant, increasing slowly (low slope) when compared with the NMSE slope for the range $5 \leq K \leq 20$.
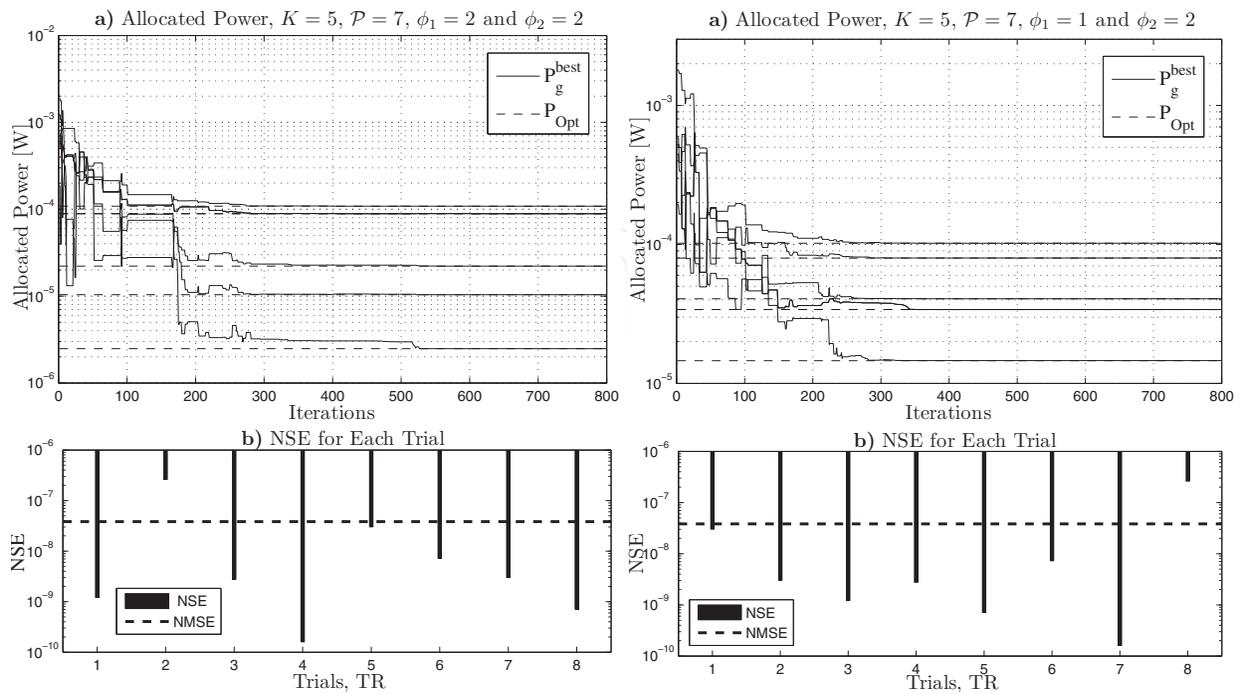
---

[12] Or instantaneous NMSE.

Fig. 20. Typical power convergence (**a**), NSE and NMSE (**b**). Random P_{initial} and channel realization for $K = 5$ users swarm power optimization. Same channel conditions throughout the $T = 10$ trials. Swarm population size, $M = K + 2$. Multi-rate case. Left) $\phi_1 = \phi_2 = 2$; Right) $\phi_1 = 1.0$, $\phi_2 = 2.0$
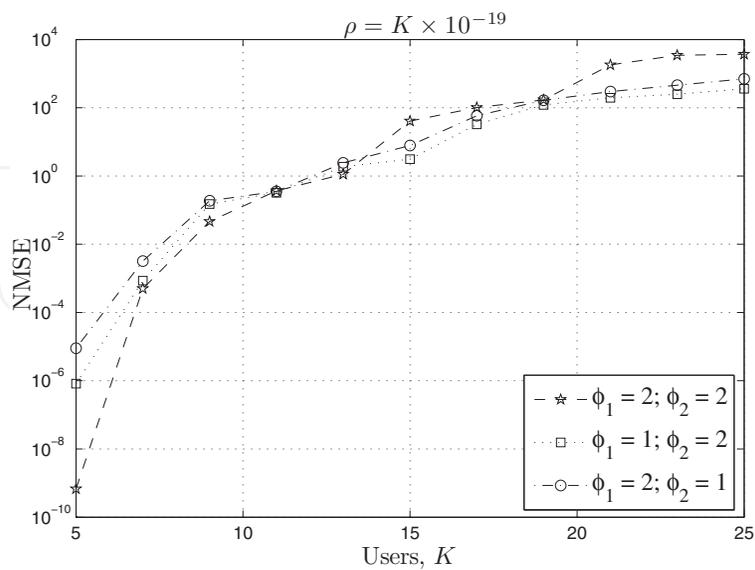

Fig. 21. Average $NMSE$ over 100 samples, $K \in [5, 25]$ for different ϕ_1 and ϕ_2. Multi-rate scenarios. $N = 1000$ iterations.

On the other hand, in terms of convergence test, as defined by eq. (54), and assuming $\epsilon_1 = \epsilon_2 = 10^{-2}$, Table 8 shows that the PSO algorithm achieves faster convergence (under this criterium) with $\phi_1 = 1$ and $\phi_2 = 2$ for any $K \in [5, 20]$ users.

K multirate users	5	10	15	20
$\mathcal{G}$ Iterations	500	600	1000	1800
$\phi_1 = 1, \phi_2 = 2$	108	301	420	488
$\phi_1 = 2, \phi_2 = 1$	127	479	526	696
$\phi_1 = 2, \phi_2 = 2$	263	591	697	757

Table 8. Convergence Results in Multirate Scenario, under (54) and $\epsilon_1 = \epsilon_2 = 10^{-2}$.

In conclusion, the numerical results for the power minimization with randomly user's rate assignment problem have revealed for high system loading that the best acceleration coefficient values lie on $\phi_1 = 1$ and $\phi_2 = 2$, in terms of convergence and solution quality trade-off. For low system loading the parameters choice $\phi_1 = 2$ and $\phi_2 = 2$ results in the best solution quality.

3.3.2.2 Power allocation overhead regards to ϕ_1 and ϕ_2

In order to corroborate the best values choice for the acceleration factors, Figure 22 shows the total system power allocation under typical channel situations, i.e., deep fading, as a function of number of multirate users, parameterized by ϕ_1 and ϕ_2. The algorithm performance in terms of minimal total power consumption for $K > 13$ is achieved with $\phi_1 = 1.0$ and $\phi_2 = 2.0$. As already mentioned, other combinations of ϕ_1 and ϕ_2 results in higher total power consumption.
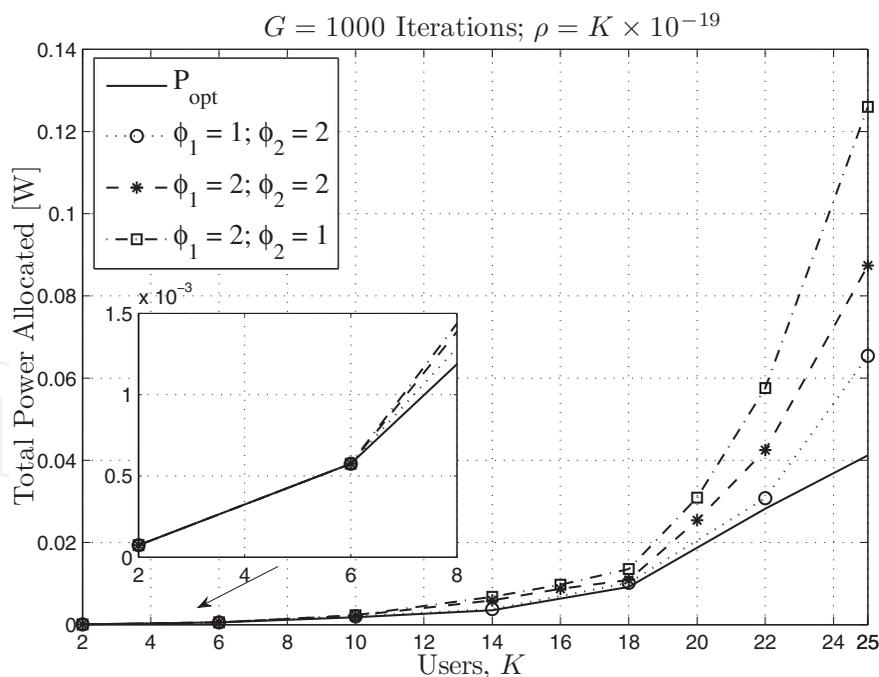

Fig. 22. System power allocation for different ϕ_1 and ϕ_2 parameters. $K \in [2, 25]$, 1000 iterations limit, Single Rate case with $R_{\min} = \frac{1}{128} R_c$.

3.3.2.3 ρ Optimization

The parameter ρ in cost function (41), was set as a function of the number of users K, such that $\rho = K \times 10^{-19}$. This relation was found based on the value suggested in Elkamchouchi et al. (2007) and adapted for the power-rate allocation problem through an non-exhaustive search. For different number of users, Figure 23 indicates the evolution of the standard deviation of the hypothetical received power vector, σ_{rp}, given by the PSO solution at the Nth iteration multiplied by the respective channel gain, $\mathbf{p}_g^{\mathrm{best}} \operatorname{diag}(\mathbf{G})$. The σ_{rp} results of Figure 23 were obtained averaging over 1000 initial swarm population (admitted uniformly distributed over $[P_{\min}; P_{\max}]$) and a single channel realization. Hence the σ_{rp} values give us a good idea about the received power disparities (near-far reduction) when the swarm optimization evolves. As a consequence, the ρ values and its direct dependence (increasing) with the number of users could be established.
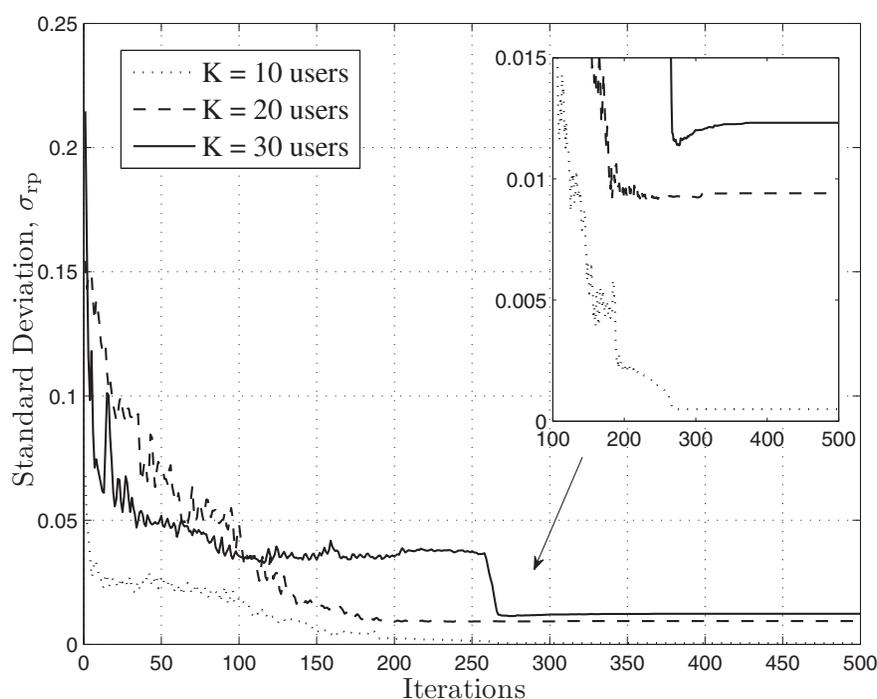
Fig. 23. Average standard deviation curves of the hypothetical received power vector, σ_{rp}, as a function of the number of iteration. Average over 1000 initial swarm population (admitted uniformly distributed over $[P_{\min}; P_{\max}]$), and single channel realization.

Figure 24 shows how hard is to solve the power allocation problem associated to the cost function in (41) on the $\mathbb{R}^K$ space. In this particular channel condition, the optimal power allocation solution and the cost function global maximum are not the same points. This happens due to the presence of users with poor channel conditions, e.g. user far away from the base station combined to deep fading channel. In this cases it is better drop the users (outage) under bad channel conditions than rise the total system power consumption to keep those users active on the system.

4. Conclusions

This chapter discusses the application of search heuristic approaches in solving different optimization problem that arise in multiple access wireless communication networks.
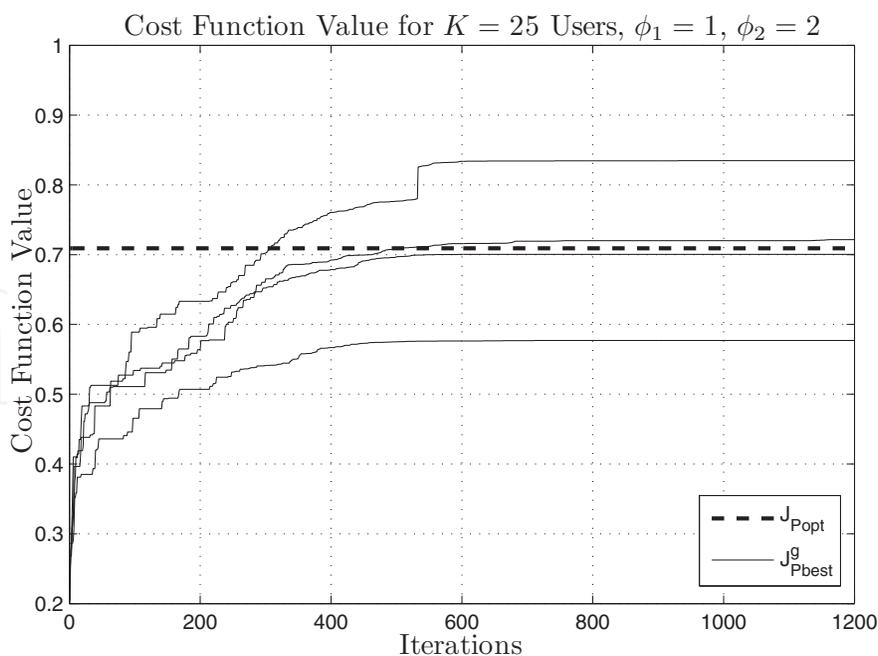
Fig. 24. Global best cost function evolution and optimal cost function value in four different samples with $\phi_1 = 1$ and $\phi_2 = 2$ parameters, $K = 25$ users, 1200 iterations limit, $\rho = K \times 10^{-19}$ and under the same channel conditions.

Specially, two optimization aspects of multiple access networks are deeply treated: multiuser detection, and simultaneous power and information rate allocation. To facing either NP optimization problem arising in multiuser detection or intrinsic non-feasibility power-rate allocation problem that appear in several practical scenarios, a discrete and continuous PSO algorithm versions are adopted and completely characterized. In both cases, the input parameters, specially the weight factors (acceleration coefficients), are optimized for each considered scenario. For both problems, extensive numerical results demonstrated the effectiveness of the proposed heuristic search approach.

Under multipath channels, different order modulations formats and antenna diversity, the PSO algorithm shown to be efficient for SISO/SIMO MuD asynchronous DS-CDMA problem, even under the increasing of number of multipath, system loading (MAI), NFR and/or SNR. Under a variety of analyzed realistic scenarios, the performance achieved by PSO-MuD always was near-optimal but with much lower complexity when compared to the OMuD, even under moderate channel errors estimation. In all evaluated system conditions, PSO-MuD resulted in small degradation performance if those errors are confined to 10% of the true instantaneous values.

Furthermore, under realistic and practical systems conditions, the PSO-MuD results in much less computational complexity than OMuD. The PSO-MuD, when compared to the CD receiver, is able to reach a much better performance with an affordable computational complexity. This manageable complexity depends on the hardware resources available and the system requirements such as minimum throughput, maximum admitted symbol-error-rate, and so on.

Besides, the PSO-MuD DS-CDMA accomplishes a flexible performance complexity trade-off solutions, showing to be appropriate for low and high-order modulation formats, asynchronous system, as well as multipath channels and spatial diversity scenarios. The

increasing system loading slightly deteriorates the performance of the swarm multiuser detector, but only under higher-order modulation. In all other scenarios, PSO-MuD presents complete robustness against MAI increasing.

For resource allocation optimization problem, numerical results indicated that searching for the global optimum over a high dimension power-rate allocation problem is a hard task. The search universe is denoted as $\mathbb{R}^K$ and constrained by power, rate and SNR ranges. Since the search space is continuous one can concludes that there is an infinite number of solutions, even if all these solutions are constrained.

The simulations results revealed that the proposed PSO approach can be easily applied to the throughput maximization problem under power consumption constraint in a large multirate system loading and realistic fading channel conditions. The algorithm has been found robust under a high number of active users in the systems, namely $K \geq 200$, while held the efficient searching feature and quality solutions. Those features make the PSO resource allocation approach a strong candidate to be implemented in real multiple access networks.

Further work and directions include a) the discretization of the search space aiming to reduce the problem dimension and, as a consequence, the complexity order; b) the application of the heuristic optimization techniques to solve resource allocation problems under a multi-objective optimization perspective; and c) the analysis of power and rate allocation problems under dynamic channels condition.

5. References

Abrão, T., de Oliveira, L. D., Ciriaco, F., Angélico, B. A., Jeszensky, P. J. E. & Palacio, F. J. C. (2009). S/mimo mc-cdma heuristic multiuser detectors based on single-objective optimization, *Wireless Personal Communications* .

Castoldi, P. (2002). *Multiuser Detection in CDMA Mobile Terminals*, Artech House, London, UK.

Chatterjee, A. & Siarry, P. (2006). Nonlinear inertia weight variation for dynamic adaptation in particle swarm optimization, *Computers & Operations Research* 33(3): 859–871.

Ciriaco, F., Abrão, T. & Jeszensky, P. J. E. (2006). Ds/cdma multiuser detection with evolutionary algorithms, *Journal Of Universal Computer Science* 12(4): 450–480.

Dai, J., Ye, Z. & Xu, X. (2009). Power allocation for maximizing the minimum rate with qos constraints, *Vehicular Technology, IEEE Transactions on* 58(9): 4989 –4996.

Eberhart, R. & Shi, Y. (2001). Particle swarm optimization: developments, applications and resources, *Proceedings of the 2001 Congress on Evolutionary Computation*, Vol. 1, pp. 81–86.

Elkamchouchi, H., EIragal, H. & Makar, M. (2007). Power control in cdma system using particle swarm optimization, *24th National Radio Science Conference*, pp. 1–8.

Elmusrati, M., El-Sallabi, H. & Koivo, H. (2008). Applications of multi-objective optimization techniques in radio resource scheduling of cellular communication systems, *IEEE Transactions on Wireless Communications* 7(1): 343–353.

Elmusrati, M. & Koivo, H. (2003). Multi-objective totally distributed power and rate control for wireless communications, *The 57th IEEE Semiannual Vehicular Technology Conference, VTC'03-Spring*, Vol. 4, pp. 2216–2220.

Ergün, C. & Hacioglu, K. (2000). Multiuser detection using a genetic algorithm in cdma communications systems, *IEEE Transactions on Communications* 48: 1374–1382.

Foschini, G. & Miljanic, Z. (1993). A simple distributed autonomous power control algorithm and its convergence, *IEEE Transactions on Vehicular Technology* 42(4): 641–646.

Gross, T. J., Abrão, T. & Jeszensky, P. J. E. (2010). Distributed power control algorithm for multiple access systems based on verhulst model, In Press, Corrected Proof: –.

Jeruchim, M. C., Balaban, P. & Shanmugan, K. S. (1992). *Simulation of Communication Systems*, Plenum Press, New York.

Juntti, M. J., Schlosser, T. & Lilleberg, J. O. (1997). Genetic algorithms for multiuser detection in synchronous cdma, *Proceedings of the IEEE International Symposium on Information Theory*, p. 492.

Kennedy, J. & Eberhart, R. (1995). Particle swarm optimization, *IEEE International Conference on Neural Networks*, pp. 1942–1948.

Kennedy, J. & Eberhart, R. (1997). A discrete binary version of the particle swarm algorithm, *IEEE international conference on Systems*, pp. 4104–4108.

Kennedy, J. & Eberhart, R. C. (2001). *Swarm Intelligence*, first edn, Morgan Kaufmann.

Khan, A. A., Bashir, S., Naeem, M. & Shah, S. I. (2006). Heuristics assisted detection in high speed wireless communication systems, *IEEE Multitopic Conference*, pp. 1–5.

Lee, J.-W., Mazumdar, R. R. & Shroff, N. B. (2005). Downlink power allocation for multi-class wireless systems, *IEEE/ACM Transactions on Networking* 13(4): 854–867.

Li Ping Qian, Ying Jun Zhang, J. H. (2009). Mapel: Achieving global optimality for a non-convex wireless power control problem, *IEEE Transactions on Wireless Communications* 8(3): 1553–1563.

Lim, H. S. & Venkatesh, B. (2003). An efficient local search heuristics for asynchronous multiuser detection, *IEEE Communications Letters* 7(6): 299–301.

Moshavi, S. (1996). Multi-user detection for ds-cdma communications, *IEEE Communication Magazine* 34: 132–136.

Moustafa, M., Habib, I. & Naghshineh, M. (2000). Genetic algorithm for mobiles equilibrium, MILCOM 2000. 21st Century Military Communications Conference Proceedings.

Moustafa, M., Habib, I. & Naghshineh, M. (2001a). Wireless resource management using genetic algorithm for mobiles equilibrium, *Computer Networks* 37(5): 631–643.

Moustafa, M., Habib, I. & Naghshineh, M. (2001b). Wireless resource management using genetic algorithm for mobiles equilibrium, Sixth IEEE Symposium on Computers and Communications. Proceedings.

Nedjah, N. & Mourelle, L. M. (2006). *Swarm Intelligent Systems*, Springer, Springer-Verlag Berlin Heidelberg.

Oliveira, L. D., Abrão, T., Jeszensky, P. J. E. & Casadevall, F. (2008). Particle swarm optimization assisted multiuser detector for m-qam ds/cdma systems, *SIS'08 - IEEE Swarm Intelligence Symposium*, pp. 1–8.

Oliveira, L. D., Ciriaco, F., Abrão, T. & Jeszensky, P. J. E. (2006). Particle swarm and quantum particle swarm optimization applied to ds/cdma multiuser detection in flat rayleigh channels, *ISSSTA'06 - IEEE International Symposium on Spread Spectrum Techniques and Applications*, Manaus, Brazil, pp. 133–137.

Oliveira, L. D., Ciriaco, F., Abrão, T. & Jeszensky, P. J. E. (2009). Local search multiuser detection, *AEÜ International Journal of Electronics and Communications* 63(4): 259–270.

Phuong, N. T. H. & Tuy, H. (2003). A unified monotonic approach to generalized linear fractional programming, *Journal of Global Optimization* pp. 229–259.

Proakis, J. (1989). *Digital Communications*, McGraw-Hill.

Seneta, E. (1981). *Non-Negative Matrices and Markov Chains*, 2 edn, New York: Springer-Verlag.

Shi, Y. & Eberhart, R. C. (1998). Parameter selection in particle swarm optimization, *1998 Annual Conference on Evolutionary Programming*, San Diego, USA.

Uykan, Z. & Koivo, H. (2004.). Sigmoid-basis nonlinear power-control algorithm for mobile radio systems, *IEEE Transactions on Vehicular Technology* 53(1): 265–271.

Verdú, S. (1989). Computational complexity of optimum multiuser detection, *Algorithmica* 4(1): 303–312.

Verdú, S. (1998). *Multiuser Detection*, Cambridge University Press, New York.

Zhao, H., Long, H. & Wang, W. (2006). Pso selection of surviving nodes in qrm detection for mimo systems, *GLOBECOM - IEEE Global Telecommunications Conference*, pp. 1–5.

Zielinski, K., Weitkemper, P., Laur, R. & Kammeyer, K.-D. (2009). Optimization of power allocation for interference cancellation with particle swarm optimization, *IEEE Transactions on Evolutionary Computation* 13(1): 128–150.
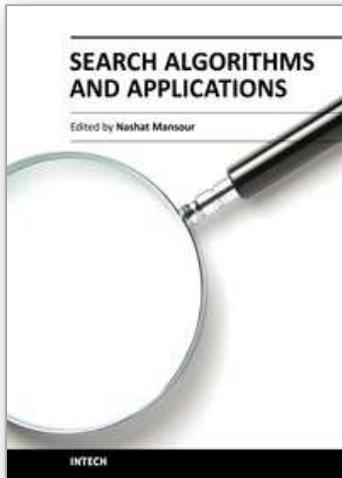
Search Algorithms and Applications

Edited by Prof. Nashat Mansour

Search algorithms aim to find solutions or objects with specified properties and constraints in a large solution search space or among a collection of objects. A solution can be a set of value assignments to variables that will satisfy the constraints or a sub-structure of a given discrete structure. In addition, there are search algorithms, mostly probabilistic, that are designed for the prospective quantum computer. This book demonstrates the wide applicability of search algorithms for the purpose of developing useful and practical solutions to problems that arise in a variety of problem domains. Although it is targeted to a wide group of readers: researchers, graduate students, and practitioners, it does not offer an exhaustive coverage of search algorithms and applications. The chapters are organized into three parts: Population-based and quantum search algorithms, Search algorithms for image and video processing, and Search algorithms for engineering applications.

How to reference

In order to correctly reference this scholarly work, feel free to copy and paste the following:

INTECH
open science | open minds